Cambridge Prisms: Drylands

www.cambridge.org/dry

Quaternary dryland dynamics: perspectives and prospects

Abi Stone

Department of Geography, The University of Manchester, M13 9PL, UK

Review

Cite this article: Stone A (2025). Quaternary dryland dynamics: perspectives and prospects. *Cambridge Prisms: Drylands*, **2**, e9, 1–16 https://doi.org/10.1017/dry.2025.10003

Received: 11 January 2025
Revised: 25 April 2025
Accepted: 26 June 2025

Keywords:
drylands; Quaternary; environmental reconstruction; climate change; hominins

Corresponding author:
Abi Stone;
Email: abi.stone@manchester.ac.uk

Abstract

Reconstructing Quaternary-timescale environmental change in drylands provides insights into styles and rates of change in response to direct insolation forcing and variations in global temperature, ice volume and sea level. Changes to the relatively inhospitable environments presented by drylands are also central to debates about the migration and adaptability of hominin species. This review outlines approaches used for reconstructing past environments, which use dated sequences of environmental proxies – the properties of physical sediments, chemical precipitates and biological materials. In addition, climate model simulations can explore responses to known climatic forcing factors. Advances in both approaches remain situated within conceptual frameworks about dryland responses to: (i) cyclical changes in the Earth's orbit around the sun, either mediated via the global cryosphere during glacial–interglacial cycles (~100 ka periodicity during the last ~0.9 Ma), or mediated via the response of the global monsoon with ~23 ka periodicity (precession) and (ii) millennial-scale climatic shifts, which are thought to originate outside drylands, within the North Atlantic.

In this review, three examples are outlined to demonstrate areas of emerging consensus and remaining contradictions: (1) speleothem and tufa growth records that span hundreds of thousands of years (ka), (2) conditions at the last glacial maximum (LGM) and (3) proxies recording millennial-scale events. Precessional-scale forcing of the monsoon is not always observed, with apparent mediating roles from glacial boundary conditions in parts of the northern hemisphere (NH) and from interglacial boundary conditions in parts of the southern hemisphere (SH). The LGM in drylands was initially conceptualised as experiencing pluvial (wet) conditions, which shifted to a glacial aridity paradigm, and is again shifting to a pattern of global heterogeneity, in which some drylands were wetter-than-present and others drier. However, there remain contradictions between environmental proxies and model simulations, and spatial heterogeneity is observed within many drylands. Dryland proxies that record millennial-scale events demonstrate clearly the importance of climatic teleconnections across the globe in influencing dryland hydroclimate. The records of Quaternary dryland change across a range of timescales get used alongside simulations of ecosystem response through time, hominin habitat and even hominin physiology to better understand likely hominin dispersals through dryland regions.

Impact statement

Dryland environments have undergone significant change during the Quaternary Period (2.58 Ma), offering a crucial long-term perspective on the climatic, environmental and ecological conditions observed today. This period is also central to understanding the large-scale impact of dryland climatic change on hominins, including the drivers for migration and evidence for adaption to aridity. This review paper presents an overview of the approaches taken to reconstruct environmental conditions and to simulate climatic changes. The paper uses three key examples that exemplify advancements in the field, which illustrate evolving interpretations, significant developments in thought, and areas where uncertainty persists. The paper emphasizes the complexity and variability of dryland changes – both across different regions and within individual landscapes – evident in both reconstructions and model simulations. In its final section, the review explores recent progress in understanding how hominins responded to climatic and environmental shifts in drylands during the Quaternary. The interplay between environmental change and hominin adaptation, migration, and evolution is currently revitalizing this area of dryland research.

Introduction

Reconstructing the past in drylands is important for three key reasons. First, geomorphological processes operating today are influenced by the landscape features inherited from the past, including the Quaternary past (~2.58 Ma). For example, the emplacement and migration of dunes during the Quaternary influence modern-day surface hydrology, such as dune damming

© The Author(s), 2025. Published by Cambridge University Press. This is an Open Access article, distributed under the terms of the Creative Commons Attribution-NonCommercial-NoDerivatives licence (http://creativecommons.org/licenses/by-nc-nd/4.0), which permits non-commercial re-use, distribution, and reproduction in any medium, provided that no alterations are made and the original article is properly cited. The written permission of Cambridge University Press must be obtained prior to any commercial use and/or adaptation of the article.

Downloaded from https://www.cambridge.org/core. UNIVERSIDAD AUTONOMA METROPOLITANA, on 19 Nov 2026 at 18:47:39, subject to the Cambridge Core terms of use, available at https://www.cambridge.org/core/terms. https://doi.org/10.1017/dry.2025.10003

during flash-flooding as well as groundwater-fed interdune lakes (Al-Masrahy and Moutney, 2015; Liu and Coulthard, 2015), with recent dramatic examples recently observed in southeast Morocco (Egbejule, 2024). Second, it helps us to understand the range of climatic and environmental conditions drylands can (or have) experience(d), which provides important context for the post-industrial period and changes predicted for the future. Reconstructions using landforms and sediments progress alongside numerical model simulations, which are valuable for exploring the influence of driving forces of past climate change in drylands, although model performance is evaluated using palaeoenvironmental data from reconstructions, reminding us of the need to examine their ability to simulate past climates realistically (e.g. Otto-Bliesner et al., 2017). Thirdly, spatio-temporal changes to aridity are central to endeavours to understand hominin evolutionary transitions (e.g. Timmerman et al., 2022), particularly abilities to tolerate dry conditions. Climate-induced changes to habitat can be simulated in order to test hypotheses about hominin evolution and migration across dryland regions.

Quaternary dryland research is a major sub-topic within dryland science, and this review aims to outline the approaches taken to reconstruct the past. In doing so, it aims to provide some critique of the current state of knowledge production and set out key areas of progress and continued debate, rather than attempt a comprehensive review of Quaternary environmental change for all major dryland regions, which would require an extensive treatment beyond the scope of a short overview. The paper briefly outlines: (1) the range of environmental data used within those reconstructions and some key numerical models used to simulate the past and (2) the dominant frameworks for global climatic change during the Quaternary. These frameworks are organised into different timescales that inherently reflect the climatic drivers, such as periodic variations in the Earth's orbit around the sun and the behaviour of the global cryosphere. I then (3) use illustrative examples to explore the status of understanding of Quaternary dryland environments, which also helps demonstrate how #2 has guided interpretations. A combination of conceptual frameworks, proxy data and model simulations is used by researchers to construct arguments, and therein, whilst we can see examples where some consensus is emerging, interpretations and reasoning often get complicated, and debates remain. The final section (4) examines a major motivation for current Quaternary dryland research, concerned with aridity as a factor likely to constrict hominin migration and/or influence adaptability.

Sources of evidence and numerical climate model simulations

To appreciate where our understanding of Quaternary environmental change in drylands comes from, we must acknowledge a range of archives (such as marine basin sediments and a range of terrestrial settings) and proxies (sedimentary, chemical and biological properties that have recorded a response to past environmental conditions) (Table 1). Environmental reconstruction uses abductive reasoning (Inkpen and Wilson, 2009), looking at changes in that proxy record through time to infer the past conditions under which it formed. This process is inherently imperfect, and whilst some signals can be statistically transformed into quantitative estimates of temperature, precipitation and salinity etc., many give qualitative information about warmer or colder, or higher or lower moisture availability.

The study of Quaternary climatic change in drylands is not solely proxy-data driven, with ideas generated from conceptualising how variations in global-scale temperature and circulation patterns may have driven the hydroclimatic conditions in drylands. For example, Jamieson (1863), Passarge (1904) and Flint (1959) argued for dryland 'pluvial' conditions during glaciations, based partly on lower temperatures favouring a higher moisture balance, whilst Sarnthein (1977) argued that lower sea-surface temperatures during glacials drove continental aridity, alongside the wind patterns tending to outflow from continental surfaces (Manabe and Hahn, 1977).

Numerical modelling simulations also advance our understanding of Quaternary dryland dynamics, allowing us to explore how drylands respond to a range of climatic drivers, or boundary conditions, such as the orbital parameters that control Earth's receipt of insolation, greenhouse gas concentrations, global terrestrial ice cover, sea-level and meltwater fluxes. This includes simulations of global aridity (e.g. Greve et al., 2017) and targeted simulations of dryland regions (e.g. Liu et al., 2021). These may be conducted for individual time-slices, such as the global LGM or the mid-Holocene, undertaken as transient simulations through time, or targeted to explore potential climatic teleconnections to a known discrete forcing event (see Table 1).

Frameworks of Quaternary climatic change

Orbital cycles

The influence of changes to Earth's orbit on glacial–interglacial cycles of the Quaternary, linked predominantly to the cryosphere in the Northern Hemisphere (NH), is well established (e.g. Milankovitch, 1920; Hays et al., 1976; Ruddiman, 2006). The varying eccentricity of the elliptical-shaped orbit influences total solar insolation receipt with quasi-regular cycles of ~400 ka and ~100 ka. The other two cycles relate to seasonality of the receipt of insolation: (i) the change in the degree of the title of the Earth (obliquity) influences the intensity of season in both hemispheres (~41 ka), whilst (ii) the direction the Earth's axis points in space, combined with the rotation of the elliptical orbit around the Sun, influences the relative strength of seasons in each hemisphere via the precession of the equinoxes (~23 ka). The pacing of global glacial–interglacial cycles, inferred from marine oxygen isotope stratigraphy (MIS), starts as ~41 ka cyclicity (e.g. Pisias and Moore, 1981; Ruddiman et al., 1986; Raymo et al., 1990), transitioning during 1.25–0.7 Ma to ~100 ka cyclicity. In MIS, even numbers are glacials and odd numbers are interglacials (Figure 2A). The ~41 ka cyclicity is thought to relate to direct obliquity forcing, involving feedbacks with atmospheric greenhouse gases, whilst the ~100 ka cyclicity cannot be accounted for by the small total insolation variations related to eccentricity (Ruddiman, 2006). Notwithstanding the debates about the nature of the forcing-cryosphere response, and the role of internal forcing and ocean-atmospheric reorganisations in the climate system (e.g. Broecker and Denton, 1989; Berger, 2013), the large change to the Earth's climatic state during these glacial–interglacial cycles is likely to have influenced the terrestrial dryland regions.

The way conditions in drylands have been conceptualised over global glacial–interglacial periods has gone through large changes in thought. There was a widespread shift in the idea of dryland pluvials during glacial periods to dryland aridity, aided by the advent of chronological control for some proxies (e.g. Williams, 1975; Sarnthein, 1977). This 'glacial aridity paradigm' was lent support by the timing of higher volumes of dust volumes in the Antarctic ice cores such as Vostok during glacials, and larger particles in the LGM layers (Petit et al., 1999), and back to 800 ka

Downloaded from https://www.cambridge.org/core. UNIVERSIDAD AUTONOMA METROPOLITANA, on 19 Nov 2026 at 18:47:39, subject to the Cambridge Core terms of use, available at https://www.cambridge.org/core/terms. https://doi.org/10.1017/dry.2025.10003

Table 1. Archives and their proxies for past climatic and environmental conditions in drylands, giving an overview of archives and their proxies for past climatic and environmental conditions in drylands, and key modelling simulations from which changes in dryland aridity can be inferred. (abbreviations are used: N – north, N-cen – north central, NW – northwest, S – south, Sn – southern, W – West, Wn – western, Kal – Kalahari)

Archive					
	Proxy types				
Location	Sediment/biological	Landform	What these indicate	Example locations	References
Marine	Terrestrial dust, including diatomite-rich	NA	Adjacent terrestrial dryland sufficiently dry to provide available sediment, and wind speeds sufficiently high and in an off-shore direction to reach the marine sediment archive.	Red Sea, Arabian Sea, Indian Ocean (Arabian Peninsula) Sn Atlantic (Namib, Kalahari) North Atlantic (Sahara)	Roberts et al. (2011), Clemens and Prell (2003), Zhou et al. (2024), Stuut et al. (2002), Parmenter and Folger (1974), Skonieczny et al. (2019)
	Terrestrial-derived pollen and charcoal	NA	Vegetation change	Southern Atlantic (Namib, Kalahari(?))	Shi et al. (2001), Daniau et al. (2023)
	Terrestrial leaf-waxes	NA	$\delta^{13}C$ for plant photosynthetic pathway type, δD_{wax} recording shifts from aridity to higher precipitation	Horn of Africa (Sahara). Sn Atlantic (Namib, Kalahari Arabian Peninsula & Thar Desert, India	Tierney and deMenocal (2013), Collins et al. (2014), Jha et al. (2024).
	Sapropels	NA	Variability of flow in Mediterranean rivers, primarily the Nile	Mediterranean (North African hydroclimate)	Rohling et al. (2015)
Terrestrial	Biological: Hyrax midden	Rock shelter	$\delta^{15}N$ is a moisture availability proxy. $\delta^{13}C$ + pollen records vegetation change.	Western Namibia and South Africa	Chase et al. (2019)
	Phytoliths	NA	Vegetation change	Australasia. Great Plains, Canada.	Turnbull et al. (2023), Boyd (2005)
	Faunal remains	NA	Species distribution, insights into biomes (and biostratigraphy)	Sn Africa	Braun et al. (2013)
	Archaeological site distribution		Availability of water, construct climatic niche	Australia, NE Africa, N-cen India. Worldwide.	Williams et al. (2015), Williams (2022), Raia et al. (2020)
	Sediments	Peniplains, pediments	More + moisture balance: surface water with high erosive power.	Namibia, Sn Africa	Picart et al. (2020)
	Sediments	Alluvial fans	Facies interpretations to understand flow conditions during deposition	Arabian Peninsula	Woor et al. (2023)
	Cobbles/gravels Cemented clasts Fluvial sands/silts	River channels and floodplains	Facies interpretations to understand flow conditions during deposition	Southern Africa	Srivastava et al. (2005)
	Aeolian Sands		Buried former channels	W Sahara, North Africa Namibia, Sn Africa	Skonieczny et al. (2015), Paillou et al. (2020)
	Dry river valleys	Former river valleys	Either higher past precipitation, or higher groundwater tables (weathering & sapping).	Botswana, Sn Africa	Nash (2022a)
	Groundwater -noble gases –stable isotopes	NA	Air temperature that rainfall precipitated at and meteoric water $\delta^{18}O$ signature.	Nubian Aquifer, Nn Africa. Stampriet Artesian Basin, Sn Africa.	Edmunds et al. (1999), Abouelmagd et al. (2017), Stute and Talma (1997)
	Speleothems	Found within caves	Presence (or growth)/absence, indicating wetter/ drier $\delta^{18}O$, $\delta^{13}C$, clumped isotopes, fluid inclusions	Yemen and Oman Susah Cave, Libya. Israel. Wadi Sannur, Egypt	Fleitmann et al. (2011), Nicholson et al. (2020), Rogerson et al. (2019), Vaks et al. (2010), El-Shenawy et al. (2018)
	Tufa (calcium-carbonate)	Various tufa morphologies	Presence = sufficiently wet, $\delta^{18}O$, $\delta^{13}C$, clumped isotopes for precipitation signatures, vegetation & temperature.	California, USA. Egyptian Oases. Western Saudi Arabia.	Smith (2009), Kele et al. (2021), Stone et al. (2023)

(*Continued*)

Downloaded from https://www.cambridge.org/core. UNIVERSIDAD AUTONOMA METROPOLITANA, on 19 Nov 2026 at 18:47:39, subject to the Cambridge Core terms of use, available at https://www.cambridge.org/core/terms. https://doi.org/10.1017/dry.2025.10003

Table 1. (*Continued*)

Archive					
	Proxy types				
Location	Sediment/biological	Landform	What these indicate	Example locations	References
	Calcretes and silc-calcretes	Hardpan surface outcrops	Either pedogenic processes, or groundwater precipitation, aided by high evapotranspiration.	Sn Africa Australia	Nash (2022b), Gale et al. (2017)
	Lacustrine sediments – physical	Lake basins	Presence of water	West China	Jiang et al. (2007)
	– ecological	Lake basins	Presence of water and information about salinity, pH, oxygenation	Namib Sand Sea, Sn Africa. Worldwide	Teller et al. (1990), Gasse et al. (1997)
	Shoreline sediments	Shorelines of lake basins	Presence of water, and energy from waves and wind to build shorelines	Makgadikgadi lake systems, Sn Africa.	Burrough et al. (2009)
	Alternating sand and coarse slope debris	Sand ramps	Sedimentology and stratigraphy reveal alternating depositional environments and wet-dry shifts.	Mojave Desert, USA. Sn Namibia, Sn Africa.	Bateman et al. (2012), Rowell et al. (2017)
		Dune damming	Fluvial response to aeolian activity and vice-versa: hydroclimatic.	NW Negev, Middle East	Robins et al. (2023)
	Sand-rich sediment	Dunes	Sufficient wind and sediment supply, and 'dry enough'	Worldwide, Thar Desert, India	Telfer and Hesse (2013), Nitundil et al. (2023)
	Silty and clay-rich sands	Lunette dunes	Pan system is dry when lunette forms and required sufficient wind energy	Lake Mungo, Australia. Witpan, Sn Africa.	Jankowski et al. (2020), Telfer and Thomas (2006)
	Silt (& sand)	Loess (desert)	Wind patterns established (tectonic control pre-Quaternary). Higher accumulation rates + larger particles indicate stronger winds (e.g. East Asian Winter Monsoon) and likely more arid.	Chinese Loess Plateau. Tajikastan, Central Asia and NW China.	Guo et al. (2001, 2002), Zan et al. (2024)
Terrestrial Ice	Desert dust	NA	Presence can indicate aridity upwind and palaeowind strength.	Antarctica (SH deserts). Guliya Ice Cap, Tibet (Taklimakan Desert)	Petit et al. (1981, 1999), Beaudon et al. (2022)
Model name	Type	Time-slice or transient	Aim of study	Area modelled	
Multi-model CMIP5 ensemble	~40 climate models from 20 modelling groups.	Time-slice LGM (21 ka)	Simulating aridity for LGM and for 4x CO_2, and critiquing how aridity is defined (meteorological, atmospheric, hydrological, agro-ecological) and measured (precipitation, evapotranspiration, relative humidity, runoff, soil moisture)	Global	Greve et al. (2017)
Multi-model (PMIP3)	Uses CMIP5 (as above)	Time-slice LGM (21 ka)	Simulate how, and to what extent, LGM moisture was different compared to a pre-industrial period baseline.	Global 60°S to 60°N	Liu et al. (2018)
Multi-model (PMIP3)	Uses CMIP5 (as above)	Time-slice mid-Holocene	Examine changes in aridity and dryland distribution and the mechanisms responsible.	Global 60°S to 60°N	Liu et al. (2019)
Multi-model (PMIP3)	Uses CMIP5 (as above)	Time-slice LGM (21 ka) ad mid-Holocene (6 ka)	What conditions are simulated for 6 ka and 21 ka? Which factors drive these changes?	Arid Central Asia	Xu et al. (2020)

(*Continued*)

Downloaded from https://www.cambridge.org/core. UNIVERSIDAD AUTONOMA METROPOLITANA, on 19 Nov 2026 at 18:47:39, subject to the Cambridge Core terms of use, available at https://www.cambridge.org/core/terms. https://doi.org/10.1017/dry.2025.10003

Table 1. (*Continued*)

Archive					
	Proxy types				
Location	Sediment/biological	Landform	What these indicate	Example locations	References
LOVECLIM	Earth system model of intermediate complexity, with atmospheric, ocean, ice sheets, vegetation: and carbon/biogeochem components	Transient (125 ka)	125 ka transient model simulation (including precipitation) to quantify the effects of climate on human dispersal, using outputs to drive a human dispersal model.	Global 90°S to 90°N	Timmmerman and Friedrich (2016)
LOVECLIM	As above	Transient (250 ka)	250 ka precipitation output used to argue for humidity-driven green corridors opening for human dispersal.	Southern Africa 20°S, 22°E and 30°S, 17°E	Chan et al. (2019)
CCSM3 + land surface model	Coupled model of atmosphere, ocean, land surface, sea-ice with a central coupler	Transient (150 ka)	Simulate climate and vegetation over 140 ka in Saharo-Arabian region to provide context for early modern human dispersal	Eastern Saharan-Arabian deserts and the Levant	Kutzbach et al. (2020)
CESM1	Community Earth System Model with atmosphere, ocean, land, sea-ice and prescribed vegetation, carbon cycle ands marine ecosystems	Time-slice LGM (21 ka)	How did changes in sea level drive tropical climate change, including rainfall? Used in a study of northeast African hydroclimatic response (recorded in tufa growth record)	30°N to 30°S	Di Nezio et al. (2016) As used by Kele et al. (2021)
CESM 1.2	Community Earth System Model (Yun et al., 2023)	Transient (3 Ma)	An earth system-biome simulation to investigate the role of vegetation and ecosystem diversity on hominin adaption and migration	Global-scale land area	Zeller et al. (2023)
iTRACE	Isotope enabled transient simulations using CESM1.3	Transient (20–11 ka)	Provide a simulation of temperature and moisture balance for the LGM to evaluate hypotheses about environmental change and the archaeological record.	Australian continent	Cadd et al. (2024)
TraCE–21 ka	CCSM3 (Community Climate Model v3)	Transient, 21 ka to present	Transient simulation to assess the evolution of dryland aridity over the last 21 ka.	Global-scale land area	Liu et al. (2021)
HadCM3	Coupled atmospheric oceanic model	Response to North Atlantic freshwater (millennial events)	Testing a teleconnection between African hydroclimate and freshwater inputs into the North Atlantic.	African continent	Thomas et al. (2009)
HadCM3	Coupled atmospheric oceanic model	Transient 125 ka	Precipitation output of Davies-Barnard et al. (2017) study used	30–40°S	Weij et al. (2024)

in EPICA DomeC (Lambert et al., 2012) (Figure 2B), and marine sediments (Figure 1, s1, Figure 2C). However, higher dust concentrations do not necessarily require an expansion of drylands, being wind-driven (more turbulent atmospheric circulation) and because of a potential reduction in wet-deposition of dust owing to a globally averaged lower moisture content during cooler glacials. The marine archives also represent an average of terrestrial material received from a wide spatial area, so that spatial heterogeneity within dryland regions will not be recorded. Therefore, whilst the dryland-derived dust proxy in ice core and marine sediment archives remains an appealing record for terrestrial drylands because they cover a long timescale, capturing multiple glacial–interglacial cycles, they are insufficient for reconstructing conditions in the drylands themselves. This requires terrestrial archives and proxies.

Variations to the global monsoon system (Wang and Ding, 2008) on ~23 ka (precession) cyclicity are also well established (e.g. Kutzbach, 1981; Cheng et al., 2022). This global-scale system includes the Asian Monsoon, North African Monsoon, North American Monsoon, the Indonesian-Australian Monsoon, South African Monsoon and South American Monsoon (Wang et al., 2017), with a strong influence on the hydroclimate of neighbouring dryland regions. For example, the well-established influence of the North African Monsoon on the hydroclimatic of the Sahara, including recent 'greening' during the North African Humid Period (see deMenocal and Tierney (2012) for a brief overview). The global-scale influence of ~23 ka (precession) forcing of insolation is complicated by its occurring in antiphase between Earth's two hemispheres. This owes to the hemisphere tilting towards the Earth (experiencing summer) moving in a cycle from a short pass to a long pass around the Sun in Earth's elliptical orbit, such that for any year with a NH summer at short pass, the SH summer is at long pass, and vice versa. Therefore, insolation forcing

Downloaded from https://www.cambridge.org/core. UNIVERSIDAD AUTONOMA METROPOLITANA, on 19 Nov 2026 at 18:47:39, subject to the Cambridge Core terms of use, available at https://www.cambridge.org/core/terms. https://doi.org/10.1017/dry.2025.10003

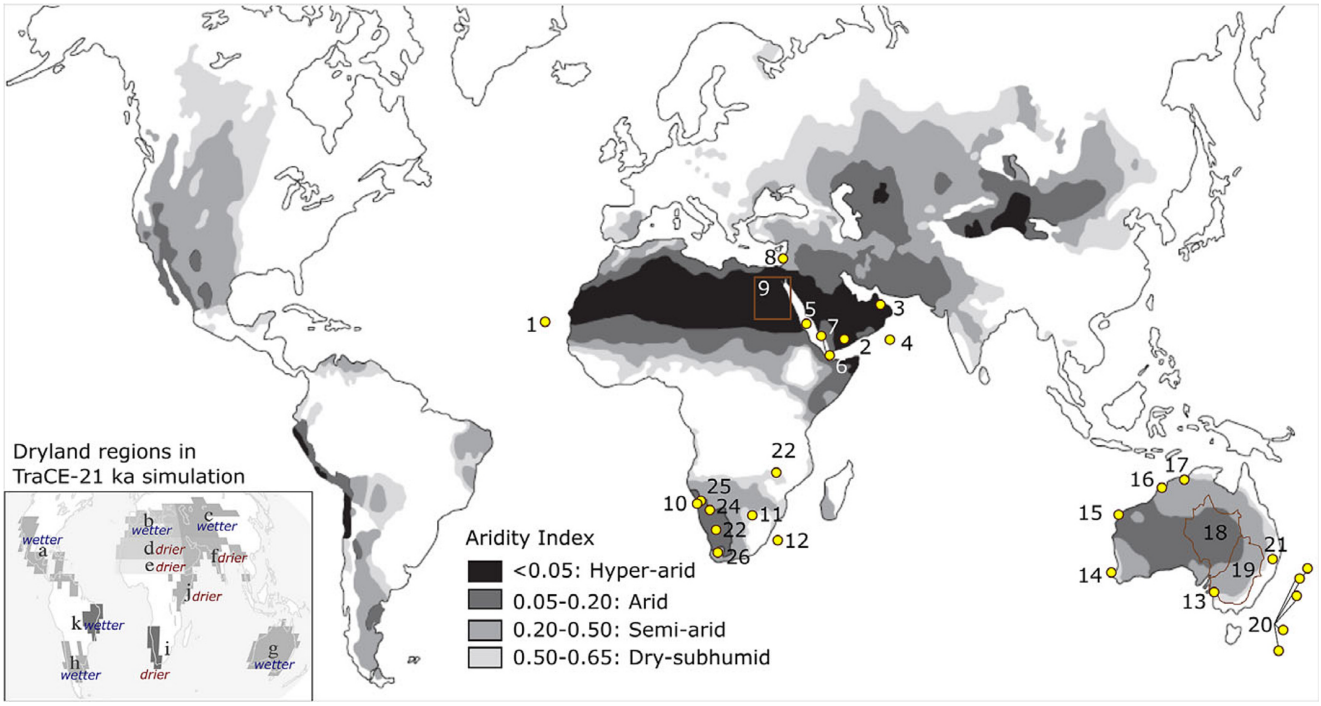


Figure 1. Map of current global dryland distribution, alongside the locations of the major proxy records explored in the three key examples in this paper and an inset of the TraCE-21 ka simulation for the LGM from Liu et al. (2021) demonstrating which dryland regions are simulated to be wetter-than-present, or drier-than-present. Site numbers (s) are referred to in the text, and (1) North Atlantic dust records, ODP659 (deMenocal, 1995), MD03–2705 and ODP659 (Skonieczny et al., 2019), (2) Mukalla Cave (Nicholson et al., 2020), (3) Hoti Cave (Nicholson et al., 2020), (4) North Arabian Sea dust record ODP721/722 (deMencoal, 1995), (5) Red Sea dust record K11 (Ehrmann et al., 2024), (6) Gulf of Aden RC09–166 (Tierney et al., 2017), (7) Wadi Dabsa tufa record (Stone et al., 2023), (8) Soreq Cave (Bar-Matthews et al., 1997), (9) Egyptian tufa growth (Kele et al., 2021), (10) Rössing Cave, Namibia (Geyh and Heine, 2014), (11) Tswaing Crater (Partridge et al., 1997), (12) CD15410–06 (Simon et al., 2015), (13) Naracoorte Caves (Weij et al., 2024), (14) Leeuwin-Naturaliste-region caves (Weij et al., 2024), (15–17) speleothems on the northwest seaboard of Australia (Denniston et al., 2017), (18) Kati Thanda-Lake Eyre Basin, (19) Murray Darling Basin, (20) Tasman Sea dust record (Hesse, 1994), (21) Native Companion Lagoon, eastern Australia (Petherick et al., 2008), (22) Lake Chilwa, Malawi (Thomas et al., 2009), (23) Pella hydrax midden (Chase et al., 2019), (24) Zizou hyrax midden (Chase et al., 2019), (25) Spitzkoppe midden (Chase et al., 2019), (26) De Rif hyrax midden (Chase et al., 2011).

is calculated and plotted for the hemisphere from which the monsoon-related response is being considered (Figure 2N shows a NH and SH summer insolation curve).

Millennial-scale variability

Climatic variability with millennial-timescale pacing was initially detected in the ice core proxies covering the last glacial (Dansgaard et al., 1972, 1982, 1993) as well as ice-rafted detritus in marine sediment cores in the North Atlantic (e.g. Heinrich, 1988), with the noticeable coincidence in timing set out by Bond et al. (1993) and Broecker (1994). Hemming (2004) considered evidence for a global climate imprint of these events and started to consider whether a connection (or teleconnection) between events had a physical basis, via ocean and atmospheric circulation. The 21 warming events from 87 to 12 ka have a quasi-periodic spacing of <2,000 years and last for 50–100 years (Wolff et al., 2010; Rousseau et al., 2017). Millennial events with a similar 1470 ± 500-year cyclicity have also been observed in the Holocene (11.7 ka) in the North Atlantic (Bond et al., 1997), although the magnitude of the variations is higher with larger ice sheets. The 'agitation' to the climate system provided by millennial-scale variability may have a role in glacial–interglacial transitions (e.g. Hodell and Channell, 2016). In order to explore potential teleconnections between NH high-latitude driven millennial events and low-latitude dryland climatic responses, numerical climate model simulations can be used.

Example 1: the timing of dryland speleothem (and tufa) growth.

Speleothem and tufa growth in drylands are good indicators for reductions in aridity (Table 1), with uranium-series dating allowing scientists to constrain their growth records over multiple 100 ka cycles. This makes them a useful archive to explore both glacial–interglacial cycles and precession forcing of the monsoon as drivers of Quaternary climate change in drylands.

On the Arabian Peninsula, the discontinuous Mukalla and Hoti Cave speleothems (14.917°N, 48.590°E and 23.083°N, 57.350°E) (Figure 1, s2,3) cover 1.1 Ma, with growth phases only occurring during peak interglacial and warm sub-stages during interglacials, and no growth during glacials (Nicholson et al., 2020). The record is used to delimit South Arabian Humid Periods (SAHPS) (Figure 2G), which show correspondence with other proxy records for humidity in the region (Nicholson et al., 2020) (Figure 1, s4–6, Figure 2D–F), and MIS 7 and MIS 5 interglacial tufa deposition at Wadi Dabsa (18.307°N, 41.564°) (Stone et al., 2023) (Figure 1, s7, Figure 2I). The conceptual explanation for the absence of speleothem growth during glacial periods is that glacial boundary conditions 'dampen' monsoon strength. More specifically, large NH high-latitude ice sheets influenced atmospheric circulation, preventing on-land penetration of the summer monsoon (Burns et al., 2001; Fleitmann et al., 2011). A role for precession-forcing seems less conclusive – there is not a SAHP for every peak in insolation (at 15°N) even during an interglacial (the non-dampened state) (Nicholson et al., 2020).

Records of speleothem growth in the Negev Desert, adjacent to the Arabian Peninsula, do not align strictly with interglacials, suggesting glacial–interglacial forcing of aridity-humidity may not be widespread across NH drylands. The ~200 ka Soreq Cave

Downloaded from https://www.cambridge.org/core. UNIVERSIDAD AUTONOMA METROPOLITANA, on 19 Nov 2026 at 18:47:39, subject to the Cambridge Core terms of use, available at https://www.cambridge.org/core/terms. https://doi.org/10.1017/dry.2025.10003

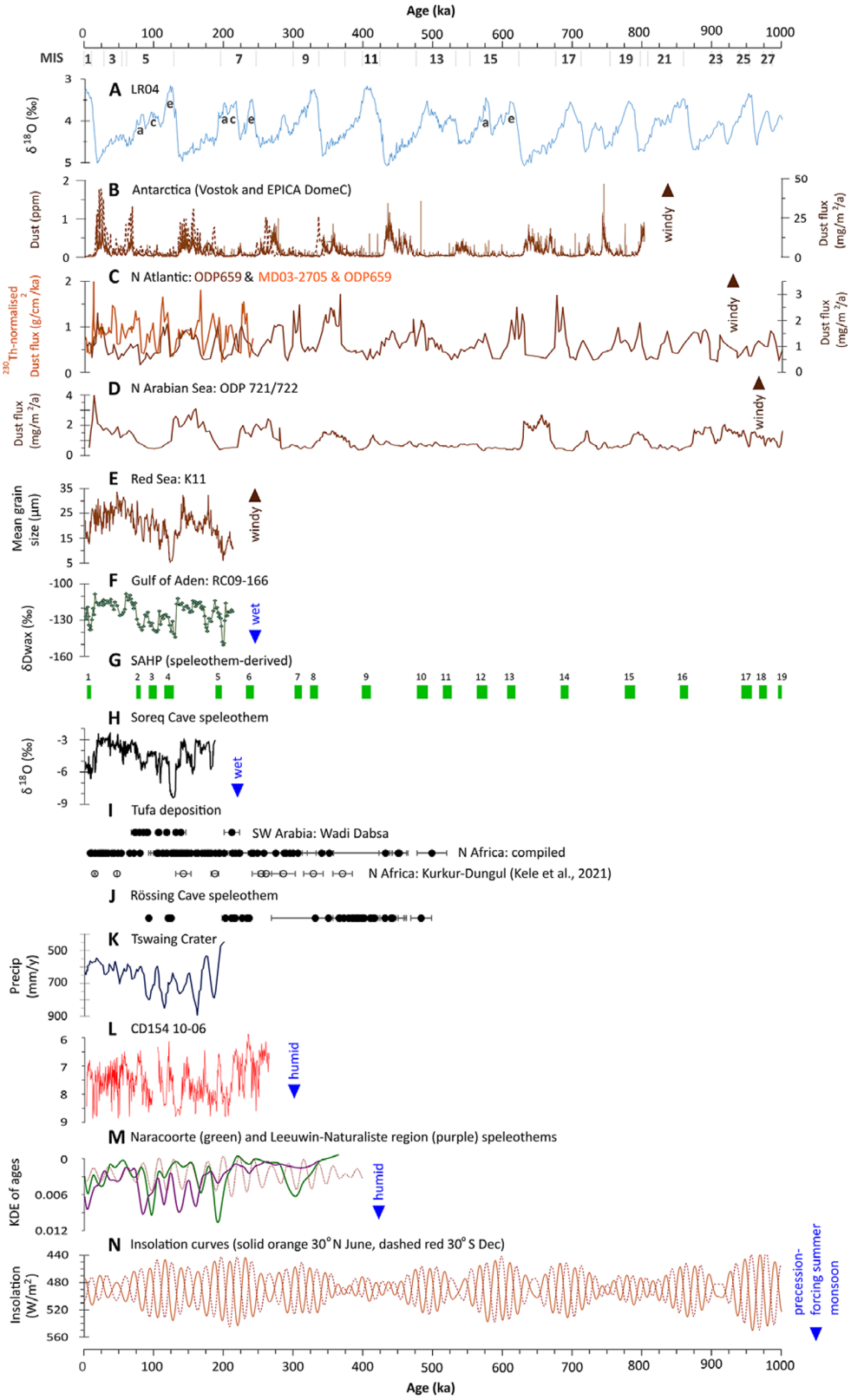


Figure 2. Key proxy records globally and for drylands, where: (A) the LR04 oxygen isotope record, with Marine Oxygen Isotope Stages (MIS) above (Lisiecki and Raymo, 2005), (B) Antarctica Vostok (Petit et al., 1999) and EPICA DomeC (Lambert et al., 2012) dust records, (C) North Atlantic dust records, ODP659 (deMenocal, 1995) and ^{230}Th corrected MD03–2705 and ODP659 (Skonieczny et al., 2019) (sites near 1), (D) North Arabian Sea dust record ODP721/722 (deMencoal, 1995) (site 4), (E) Red Sea dust record K11 (Ehrmann et al., 2024) (site 5), (F) Gulf of Aden RC09–166 terrestrial leaf wax δD (Tierney et al., 2017) (site 6), (G) speleothem-growth record derived South Arabian Humid Periods (SAHPS) (Nicholson et al., 2020) (sites 2 and 3), (H) Soreq Cave δ^{18}O record (Bar-Matthews et al., 1997) (site 8), (I) Tufa growth records from Wadi Dabsa, SW Arabia (Stone et al., 2023) (site 7) and N Africa (summarised in Kele et al., 2021) (within box 9), (J) Rössing Cave speleothem growth record (Geyh and Heine, 2014) (site 10), (K) Tswaing Crater rainfall proxy (Partridge et al., 1997) (site 11), (L) CD154–10-06P southwest Africa humidity record derived from Fe/K ratios for highly eroded terrestrial sediment (Simon et al., 2015) (site 12), (M) KDE (Kernel Density Estimates) for speleothem U-Th ages using 5 ka bandwidth for Naracoorte (east) (site 13) and Leeuwin-Naturliste region (west) (site 14) speleothems in southern Australia (Weij et al., 2024), and (N) insolation curves for summer in each hemisphere to demonstrate precession-paced forcing, where solid orange line is 30°N June and dashed red line is 30°S December (from Laskar et al., 2004).

Downloaded from https://www.cambridge.org/core. UNIVERSIDAD AUTONOMA METROPOLITANA, on 19 Nov 2026 at 18:47:39, subject to the Cambridge Core terms of use, available at https://www.cambridge.org/core/terms. https://doi.org/10.1017/dry.2025.10003

(31.754°N, 35.021°E) $\delta^{18}O$ record (Bar-Matthews et al., 1997) (Figure 1, s8, Figure 2H), along with dated fragments across seven other caves, indicates four Negev Humid Periods (NHPs) (Vaks et al., 2010), which do not align strictly with interglacials: NHP-4 (MIS 10 into MIS 9), NHP-3 (MIS 8), NHP-2 (MIS 7), and NHP-1 (late MIS 6 into MIS 5). In examining a role for precession-paced forcing, Vaks et al. (2010) find NHPs lead NH insolation peaks by several 1,000 years, with no clear explanation. The conceptual mechanism to explain monsoon-forcing of NHPs is complicated, involving a Mediterranean Sea moisture source from synoptic cyclones and an Atlantic moisture source. For the latter, a sea-surface temperature-driven reduction of the Azores High pressure system might allow the North African Summer Monsoon (Atlantic-source) to reach as far east as the Negev (deMenocal, 1995, 2004; Bar Matthews et al., 1997).

Further west into northeast Africa, Egyptian tufa growth records also indicate deposition in glacial periods (MIS 2 to MIS 12), in addition to peak interglacials, but not with precession-pacing (Kele et al., 2021) (Figure 1, s9, Figure 2I). Kele et al. (2021) propose a mechanism for 'glacial enhancement' of moisture in Egypt rather than the 'dampening' experienced in southern Arabia. When the Sunda and Sahul shelves (Indonesia and north of Australia) are exposed as landmass during glacial lowering of sea level, reduced oceanic Indonesian throughflow leads to atmospheric circulation changes that increase rainfall over East Africa. However, whilst Kele et al. (2021) draw on the CESM1 simulation of response to that glacial sea level change to support this idea (Di Nezio et al., 2016), the simulation only demonstrates an increase in rainfall over eastern equatorial Africa, not over Egypt.

In the SH, stalagmite and flowstone growth records from Rössing Cave, Namibia (22.531°S, 14.798°) (Figure 1, s10) date to interglacials MIS 5e, MIS 7 and MIS 11, but also extend through the MIS 10 glacial (Geyh and Heine, 2014) (Figure 2J). The proposed moisture source is an expansion of summer rainfall over to the west coast of southern Africa, bringing Indian Ocean Monsoon moisture, although it is not clear why Geyh and Heine (2014) do not consider precession-paced forcing. Two key long proxy records for eastern southern Africa do reveal some precession-pacing: (i) Tswaing Crater sedimentary proxy record (25.416°S, 28.101°E) (Figure 1 s11, Figure 2K) (Partridge et al., 1997) and (ii) CD15410–06 (31.177°S, 32.159°E) (Figure 1, s12) humidity proxy based on Fe/K ratios for highly-weathered terrestrial sediment delivered to the ocean (Figure 2L) (Simon et al., 2015). This example clearly illustrates the practice of different authors with respect to using the frameworks for Quaternary climatic change – Geyh and Heine (2014, p. 381) frame their study by asking 'whether the speleothems of the cave formed during glacial or interglacial periods.'

In Australia, speleothem growth records covering ~350 ka for Naracoorte Caves (~36.95°S, 140.75°E) (Figure 1, s13) and Leeuwin–Naturaliste region caves (~33.54°S, 115.02°E) (Figure 1, s14) in the southern dryland margin, are derived from speleothem 'rubble' pieces combined into an age-frequency plot smoothed with a kernel density estimator (KDE) (Weij et al., 2024) (Figure 2M). The KDE plots demonstrate a precessional rhythm of speleothem deposition for both caves, with good coherence with the 30°S summer (Dec 21st) insolation curve (Weij et al., 2024). The absence of growth peaks in the warmest part of the last three interglacials interrupts the precession-paced pattern, which leads Weij et al. (2024) to suggest that a threshold of warmth might be crossed during peak interglacials, leading to a drop in moisture availability. We could term this an 'interglacial dampening' of moisture availability, in contrast to the 'glacial dampening' observed in the southern Arabian Peninsula. However, there is an absence of large KDE peaks in some of the glacial periods (e.g. during the two precession peaks later in MIS 8 and the final precession peak in late MIS 6 for Naracoorte and all of the precession peaks in MIS 8 for Leeuwin-Naturaliste) (Figure 2M), which requires further explanation.

Overall, the speleothem and tufa records from drylands and their margins do not straightforwardly show an anti-phased NH and SH moisture availability response predicted from precession-paced forcing of monsoons. Feasible mediating roles have emerged for either glacial or interglacial, end-member boundary conditions, with: a glacial dampening in southern Arabia, a glacial enhancement in north-east Africa and an interglacial dampening in Australia.

Example 2: (Re)assessing Last Glacial Maximum (LGM) aridity.

The Australian dryland margin speleothem record (Weij et al., 2024) is one line of evidence that challenges the 'glacial aridity paradigm' for the continent (e.g. Hesse, 1994; Miller et al., 1997; Magee and Miller, 1998). Alongside other speleothems on the north-west seaboard (Denniston et al., 2017) (Figure 1, s15–17), and proxy evidence in the Kati Thanda-Lake Eyre and Murray Darling Basins (LEB Figure 1, s18 and MDB Figure 1, s19), a continental-wide picture of an LGM without a substantial decrease in moisture balance emerges (Cadd et al., 2024). Earlier LGM proxy data syntheses have variably excluded the arid interior in their treatment (e.g. Petherick et al.'s (2013) temperate zone review), included it (e.g. De Deckker et al., 2020), or focussed solely on it (e.g. Fitzsimmons et al., 2013), demonstrating different conceptualizations of spatial heterogeneity from the point of synthesis design. Key records from which arid (and cool) conditions have been inferred include: (i) low lake levels (e.g. Harrison, 1993), (ii) wind-derived terrestrial sediment in the Tasman Sea (Hesse, 1994) (Figure 1, s20) and in lagoonal sediments (Petherick et al., 2008) (Figure 1, s21), (iii) an increased rate of dune accumulation across major desert dunefields (Hesse, 2016) and (iv) shifts in vegetation from trees to herbs and grasses (e.g. Dodson, 1975; Harle, 1997; Colhoun et al., 1999). The emerging consensus for a positive moisture balance during the LGM (De Deckker et al., 2020; Weij et al., 2024; Cadd et al., 2024) is motivation to re-examine these proxies and their interpretative frameworks.

Terrestrial dust has been critiqued as an aridity indicator (see Section title "*Introduction*"). For the LGM dune accumulation record, even before questioning whether a definitive link to aridity (and not primarily to windiness), there is a notable lack of spatial homogeneity. Whilst LGM accumulation rates are increased the Malee (Lomax et al., 2011), the wider Simpson-Strzelecki contains mixed rates, suggesting "a mosaic of bare patches of sand… and large areas of vegetated, stable surface" (Hesse, 2016, p. 26). In the case of the vegetation records, there is a growing argument that lower CO_2 during the LGM had a greater influence than any inferred changes in moisture availability (e.g. Prentice et al., 2022; Scheff et al., 2017). The lake and fluvial geomorphic records remain more enigmatic. First, there are potential spatial contrasts. In the LEB region, shorelines and basin floor sediment from Lake Callabonna-Frome and Kati Thanda-Lake Eyre indicate low or desiccated conditions, respectively, in contrast to oscillating-or-full lake conditions in the MDB region (see review by Fitzsimmons et al., 2013). Furthermore, LEB fluvial proxies (dated channel sediments and overbank sediments) yield a different hydrological record than the lake shorelines, with no discernible decrease in hydrological activity during the LGM observed in a KDE probability density curve (see Cadd et al., 2024). It is, however, sensible to

Downloaded from https://www.cambridge.org/core. UNIVERSIDAD AUTONOMA METROPOLITANA, on 19 Nov 2026 at 18:47:39, subject to the Cambridge Core terms of use, available at https://www.cambridge.org/core/terms. https://doi.org/10.1017/dry.2025.10003

apply caution to using probability density estimates on age databases from discontinuous sedimentary archives, particularly when they are not sampled using the same vertical resolution across space (e.g. Stone and Larsen, 2011). Cadd et al. (2024) also explore precipitation minus evaporation in the transient iTRACE simulation (21 to 11 ka), which shows LGM conditions had at least as great (or greater) moisture availability than the Holocene across the whole continent. This simulation contrasts with the Fast Ocean Atmospheric Model (FOAM) time-slice simulation of reduced strength Indo-Australian summer monsoon during the LGM (Marshall and Lynch, 2006) but is similar to the transient TraCE-21 ka simulation of a wetter LGM (~30% reduction in the aridity index) at the continental scale (Liu et al., 2021).

The 'glacial aridity paradigm' is also challenged in southern Africa. Two proxy syntheses indicate an area wetter than present west of ~27°E and south of ~17°S (covering the Namib Desert and most of the Kalahari), whilst the rest of the subcontinent was drier, including the eastern fringes of the Kalahari (Chase and Meadows, 2007; Gasse et al., 2008). There is no clear peak in Kalahari dune building at the LGM for any part of the last ~120 ka (Stone and Thomas, 2008), and southern Africa is the testing ground for a strong critique of dune accumulation as a proxy for inferring dryland aridity (Chase, 2009). Model simulations of LGM precipitation over southern Africa are variable and indicate either drier or wetter conditions (e.g. see Stone's (2014) discussion of outputs from HadAM3, UGAMP and PMIP2 ensemble mean and NCAR-CCM3). TraCE-21 ka simulates an ~8% higher LGM aridity index than pre-industrial conditions for Southern Africa (Liu et al., 2021). In contrast, LOVECLIM transient simulations reveals a spatial contrast, with wetter-than-present conditions in the southwest (30°S, 17°E) and drier-than-present conditions in the central-Kalahari (20°S, 22°E), which is similar in nature, but not spatial boundaries, to the proxy syntheses.

The TraCE-21 ka model provides a global-scale perspective on dryland LGM conditions, simulating wetter conditions (16% lower aridity index) compared to present, as driven by lower gas concentrations (GHG) (Liu et al., 2021). However, there is spatial heterogeneity in the simulations: (i) wetter-than present in northern American drylands, The Mediterranean, inner Asia, northeast Brazil, southern South America and Australia, and (ii) drier-than-present in eastern Africa, the Sahel, (very slightly in north Africa), west and south Asia and southern Africa (Figure 1 inset). By separating out driving factors (orbitally-driven insolation (ORB), GHG, global ice-sheets (ICE) and meltwater forcing) using multiple simulation runs (Liu et al., 2021), explanations for the regional trends can be extracted: (1) NH mid-latitude drylands (northern America, inner Asia, the Mediterranean) respond most strongly to GHG and ICE; (2) NH subtropics respond mostly to ORB (the Sahel, north Africa, west and south Asia), with LGM-dryness roughly one precession-cycle ago; (3) SH mid-latitudes (Australia, southern South America) are in tandem with the NH mid-latitudes and only increase in aridity post-LGM with reduced ICE and (4) tropical drylands (eastern Africa, northeast Brazil) are also largely driven by ICE, with lower sensitivity to ORB. Southern Africa stands out from the rest of the SH in terms of a drier LGM, and with no dominant driver. Liu et al.'s (2021) study is also a good demonstration of our current limitations in palaeomodel-proxy data comparisons. There are just 17 available hydroclimate proxies for (within, or near) 9 of the 11 dryland regions, with a maximum of two per region, and none for Australia. This greatly limits the conclusions we can draw from model-data comparisons and masks the spatial heterogeneity that is revealed in more complete proxy-data syntheses (e.g. Thomas and Burrough, 2012; Stone, 2021).

Overall, this example demonstrates a revision of the LGM aridity paradigm for both Australia and southern Africa back, although this is not necessarily a reversion to the idea of pluvial conditions, but rather conditions as wet, or slightly wetter than present. It also reveals complications and contradictions within the proxy record and between model simulations. Quaternary scientists approach these contradictions in different ways. For some, this represents a motivation to re-examine how some of the proxy records are interpreted in terms of the abductive reasoning back to climatic conditions (e.g. Chase and Meadows, 2007; Cadd et al., 2024). For others, the conclusion is that the LGM was spatially heterogeneous within dryland regions (e.g. Thomas and Burrough, 2012; Fitzsimmons et al., 2013; Stone, 2014, 2021).

Example 3: millennial-scale hydroclimatic shifts in African drylands.

Luminescence-dated shorelines of Lake Chilwa in the savannah to semi-arid climatic region of Malawi, ~15°30′S (Figure 1, s22), revealed lake highstands at 38.4–35.5, 24.3–22.3, 16.2–15.1, 13.5–12.7, 11.01 ± 0.76 and 8.52 ± 0.56 ka, (Thomas et al., 2009) (Figure 3A). The first three have a coincidence of timing with North Atlantic Heinrich Events/Stadials (HS) 4, 2 and 1, and the ~11 ka highstand with the Younger Dryas (Figure 3A). A HadCM3 climate model simulation was used to explore a potential teleconnection. It showed that a reduction of the Atlantic meridional overturning circulation in response to a North Atlantic Heinrich iceberg discharge event has atmospheric teleconnections, with increases the moisture balance at Lake Chilwa (Thomas et al., 2009) (Figure 3B). The spatial pattern in the simulation is for increased moisture balance over much of southern Africa (south of 15°S) but drier conditions north of the equator (Figure 3B). This invites future model-proxy comparisons for the African continent in response to millennial-scale climatic forcing.

Millennial-timescale change can also be examined using high-resolution (~20–30 μm/y) banded hyraceum (fossilised urine) in hyrax middens on the western margin of southern Africa. The midden record composite $\delta^{15}N$ from three dryland-zone middens (Pella, South Africa: 29.00°S, 19.14°E; Zizou: 24.07°S, 15.97°E and Spitzkoppe: 21.83°S, 15.20°E, Namibia) (Figure 1, s23–25) contains evidence of phases of increased humidity, which Chase et al. (2019) correlate with HS3, 2 and 1. De Rif midden, just south of the current dryland zone (32.446°S, 19.221°E) (Figure 1, s26), is also characterised by humid conditions during HS1 (Chase et al., 2011). Although not considered using a simulation experiment, the driving mechanism explored is an oceanic teleconnection with NH millennial events, via their influence on the southern Atlantic (Benguela upwelling zone) sea-surface temperatures (SST), and in turn the influence SSTs have on rainfall over Southern Africa's western margin. This draws on the good temporal correspondence between SST records in the South Atlantic Benguela upwelling zone (Farmer et al., 2005; Kim and Schneider, 2003) and the hyrax aridity proxies (Chase et al., 2011). However, unlike for the Chilwa Lake example, the hydroclimatic response of the De Rif midden during the YD (which also involves a North Atlantic meltwater event) is markedly different than for the HS events, with an abrupt drying signal. Chase et al. (2011) invoke an immediate atmospheric inter-hemispheric teleconnection, as opposed to the oceanic teleconnection with Benguela SST-driven hydroclimatic control for the HS events. These nuances are complex, and a paucity of continuous

Downloaded from https://www.cambridge.org/core. UNIVERSIDAD AUTONOMA METROPOLITANA, on 19 Nov 2026 at 18:47:39, subject to the Cambridge Core terms of use, available at https://www.cambridge.org/core/terms. https://doi.org/10.1017/dry.2025.10003

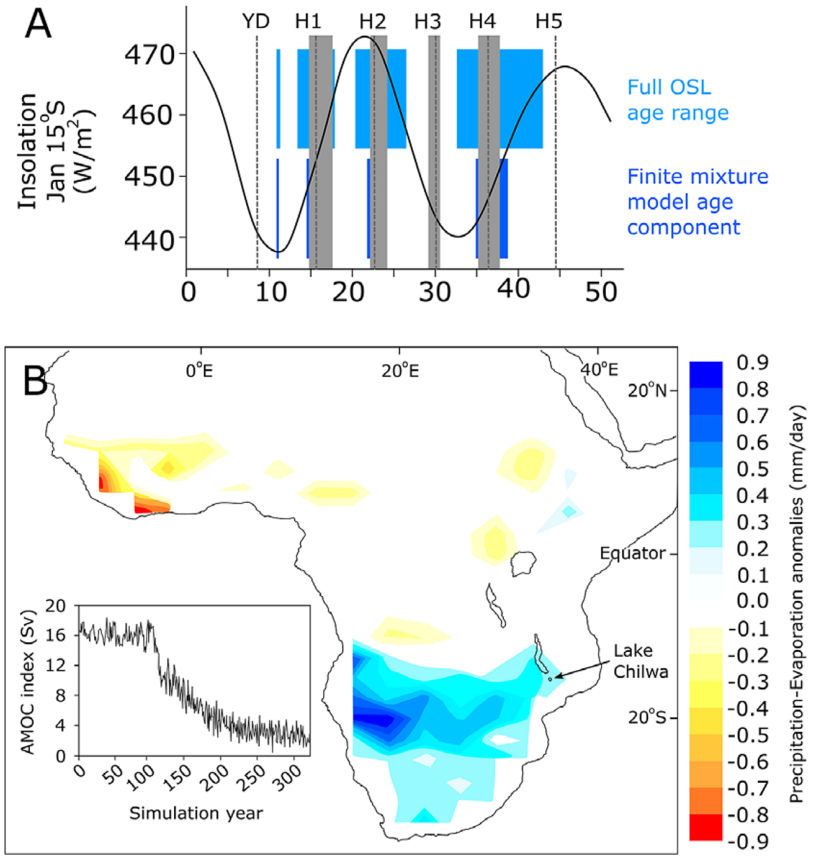


Figure 3. (A) Timing of highstands of Lake Chilwa from luminescence dating of shorelines, compared to the timing of Heinrich Events, (B) HadCM3 simulation of terrestrial moisture balance over Africa caused by a 'freshwater hosing' 50–70°N to simulate a North Atlantic Heinrich Event, displayed as an anomaly (modelled years 275–300 minus the average of 0–100 years), where the inset shows modelled reduction in Atlantic Meridional Overturning Circulation (modified from Thomas et al., 2009).

and high-resolution terrestrial proxies in African drylands restricts the possibility to test and refine these interpretations, although transient numerical model simulations for discrete spatial locations may provide further insights.

Approaches to understanding hominin response to Quaternary climate change

Understanding Quaternary climatic conditions in drylands is central to ongoing debates around which species in the *Homo* genus first possessed the adaptive capabilities to occupy hyper-arid regions. For example, Mercader et al.'s (2025) assertion that *H. erectus* adapted to a steppe-desert environment in Tanzania by utilising fluvial resources, challenging the dominant narrative that only *H. sapiens* were capable of sustained adaptations (e.g. Roberts and Stewart, 2018). Assessing the large-scale impact of dryland climatic change on hominins is made challenging by the spatially patchy and temporally punctuated nature of both the archaeological record and the terrestrial palaeo-environmental record. Improving our understanding requires continued efforts to provide environmental reconstructions with robust chronological control at the site of the archaeological evidence, in order to provide the local environmental context for those finds. Model simulations of past climates also offer an opportunity to revolutionise understanding (Timmerman et al., 2024). Early simulation attempts used multiple snapshot simulations. For example, Eriksson et al. (2012) used intervals increasing from 1 to 4 ka through the last 120 ka using the Hadley Centre model (HadCM3) to relate to the record of genetic variation in modern human populations. Increases in computational power now enable transient simulations for 120 ka (e.g. Timmerman and Friedrich (2016) using the Earth system model LOVECLIMv1.1) and even through to 3 Ma (e.g. Zeller et al. (2023) using the Community Earth System Model v1.2 (CESM1.2)) (Table 1).

Timmerman et al. (2022) use the CESM1.2 transient model simulation of the last 2 Ma, linked to a climate envelope model (CEM), to explore how changes in temperature (annual mean), precipitation (annual means and minimums) and terrestrial net primary productivity influenced the species distributions we observe in the fossil record. The CEM used topographically downscaled (1°×1°grid) average climate data for 1,000-year time windows and a species database of dated hominin fossils and lithic records (from Raia et al. (2020) and Mondanara et al. (2020)), from which species-presence locations and their associated ages were extracted. The second step derived a habitat suitability model for each species (*H. ergaster* + *H. habilis, H. erectus, H. heidelbergensis, H. neanderthalensis and H. sapiens*) (Figure 4), employing the Mahalonobis distance (a statistical approach applicable to a correlation matrix of data for the climatic variables chosen here, rather than pairs of climatic variables (Farber and Kadmon, 2003)).

The habitat suitability model reveals 'patchworks of habitable areas' (Timmerman et al., 2022, p. 500) within Earth's drylands and demonstrates that *H. sapiens* is the most tolerant species, or 'best equipped to cope with dry conditions' (p. 497) (Figure 4). This supports the idea that *H. sapiens* migrated along 'green corridors' in the dryland Saharo-Arabian belt (Larrasoaña et al., 2013; Breeze et al., 2016; Beyer et al., 2021; Groucutt et al., 2021) and supports the

Downloaded from https://www.cambridge.org/core. UNIVERSIDAD AUTONOMA METROPOLITANA, on 19 Nov 2026 at 18:47:39, subject to the Cambridge Core terms of use, available at https://www.cambridge.org/core/terms. https://doi.org/10.1017/dry.2025.10003

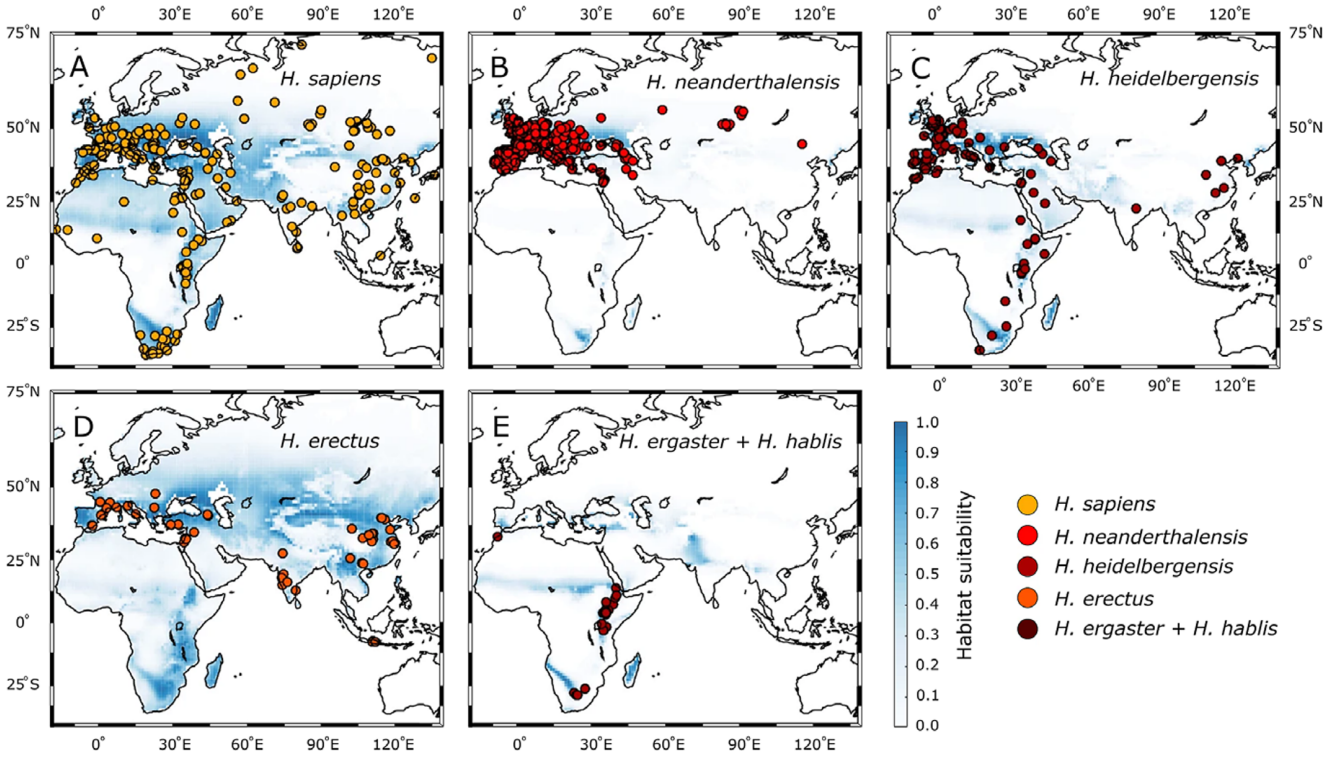


Figure 4. Hominin species distributions, expressed as time-averaged habitat suitability (intensity of blue shading) over 2 million years from Timmerman et al. (2022), also showing (with coloured circles) the locations of fossil and/or archaeological artefact evidence associated with each of the five hominin groups, collated by Timmerman et al. (2022).

idea of a multi-regional, or polycentric, origin for *H. sapiens* (Scerri et al., 2018). Furthermore, these habitable areas appear likely to have been long-term refugia for a variety of hominins within Africa (Timmerman et al., 2022), and their locations include dryland regions in both the south and north of the continent (Figure 4). Timmerman et al. (2022) also observe an orbital-timescale shift in the position of these refugia, which supports the idea that orbital forcing of the global climate was a major driving factor for hominin species distributions, and therefore also dispersal and likely also speciation (e.g. Hua and Wiens, 2013). Climatic change can also be investigated as a driver of *Homo* species extinction, for example Raia et al. (2020), use a statistical approach for the quantification of species vulnerability to climate change (climatic niche factor analysis), based on using the Planet Simulator–Grid-enabled Integrated Earth system model emulator (PALEO-PGEM) of Holden et al. (2019). Their niche analysis demonstrates a significant reduction in climatic niche space just before extinction (disappearance in the fossil record).

Conclusions

Reconstructing Quaternary conditions in drylands allows us to understand how these environments change in response to climatic forcing over a range of timescales, from the changes to Earth's orbit around the sun to the more abrupt millennial-scale cryosphere-oceanic reorganizations. This major sub-topic in dryland science progresses via environmental reconstruction and model simulation approaches, both of which are guided by conceptual frameworks for global climatic change during the Quaternary. In the former, proxy records are interpreted within the frameworks of: (i) comparing hydroclimatic conditions during glacials and interglacials, (ii) looking for precession-pacing in responses and (iii) examining any coincidences in timing with millennial-scale events that originate in the North Atlantic region along with potential teleconnections. Model simulation experiments are set up to explore the role of orbital forcing, long and short-term changes to the Earth's cryosphere with associated changes to sea levels and oceanic circulation, as well as greenhouse gas concentrations. A major motivation for Quaternary dryland research is the desire to understand how environmental changes in drylands relate to habitability limits for hominins and likely routes for migration and dispersal. After setting out approaches taken in reconstructing the Quaternary past in drylands, this review used three key examples to examine and critique progress in understanding, before outlining current and future prospects for understanding the hominin response(s) to Quaternary dryland changes.

The first example of dryland speleothem (and tufa) growth, reveals records of moisture availability that are more complicated than a precession-paced (~23 ka) control on summer monsoon rainfall, which would be antiphased between the NH and SH. Instead, there is strong glacial–interglacial overprinting with regional contrasts in its nature. In the NH, southern Arabia experienced glacial dampening of monsoon rainfall from the Indian Ocean, whilst north-east Africa experienced enhanced rainfall during glacials. In the SH, the southern Australian speleothems record is of reduced moisture availability in interglacials, likely representing a temperature threshold, whilst the Namibian record on the west coast of southern Africa shows higher moisture balance during interglacials. In the second example, a combination of proxy data (reconstructions) and model simulations demonstrates a revision of the paradigm of high aridity during the LGM in drylands. The LGM is shown to be wet, or wetter-than-present, across Australia and the west of southern Africa. However, a global-scale simulation

Downloaded from https://www.cambridge.org/core. UNIVERSIDAD AUTONOMA METROPOLITANA, on 19 Nov 2026 at 18:47:39, subject to the Cambridge Core terms of use, available at https://www.cambridge.org/core/terms. https://doi.org/10.1017/dry.2025.10003

reveals heterogeneity across space with six dryland regions wetter-than-present at the LGM, and five drier. Potential explanations for the simulated spatial patterns include different strengths of response to different climatic forcing factors (orbital parameters, the size of the global cryosphere, concentrations of greenhouse gases) in different regions, although southern Africa emerges as an outlier without a dominant driver. The LGM example also reveals that when environmental reconstructions at many sites are considered, spatial heterogeneity of environmental change within that dryland emerges. This requires us to question the usefulness of model-proxy comparisons that are based upon only one or two records of environmental change. The spatial patterns within that heterogeneity require more investigation. For example, the contrast between moisture availability in north-east Africa and Arabia over glacial–interglacial timescales and the reason for the west–east pattern of wetter versus drier for the LGM in southern Africa. It is also important to continue to critique the hydroclimatic inferences that can be made from proxies. For example, deposited dust and dune accumulation relate as much to (or more to) wind regime as they do to moisture balance. The third example of millennial-scale hydroclimatic shifts in high-resolution archives in southern Africa provides an excellent demonstration of the likely teleconnections between dryland climates and the North Atlantic during high magnitude changes to the cryosphere-ocean–atmosphere system.

All three examples demonstrate a complexity of regional and local patterns of Quaternary environmental change within drylands, of which many details remain to be fully understood. The heterogeneity revealed across space from terrestrial proxy records is a reminder of the importance of moving beyond marine archives for terrestrial dryland environmental conditions that accumulate a spatially-averaged record of sediments derived from the neighbouring continental land mass. Therefore, site-specific studies of past environmental conditions are central to refining our understanding and importantly are at the heart of understanding the environmental conditions experienced by hominins in the landscapes they were inhabiting. Approaches to understanding hominin interactions with dryland environmental change are also driven forward by model simulation approaches, including simulations of habitat suitability. These suggest that it is likely *H. sapiens* were the most tolerant to dry conditions and able to utilise patchworks of habitable areas, with some habitable areas operating as long-term refugia and others as shorter-lived 'green corridors' for migration and dispersal (Timmerman et al., 2022). However, recent environmental reconstructions in Tanzania suggest that earlier members of the *Homo* genus may have also possessed ecological flexibility, such as *H. erectus* utilising dryland water sources and demonstrating adaption to steppe-desert conditions (Mercader et al., 2025). Quaternary dryland research has both a rich history and an exciting future.

Acknowledgements. Thank you to Cambridge Prisms: Drylands for the invitation to write a review article, and funding from the University of Manchester for a Manchester-Melbourne Research Fund Grant 'A Southern Hemisphere perspective on human-environment relations along desert margins,' which provided time on a research trip to Melbourne to develop the basis for this review. Also thanks a wide range of colleagues in Quaternary Drylands for informative and supportive discussions about these themes over the years and to three anonymous reviewers for their insightful critiques, which greatly improved the overall message, structure and scope of this review.

Financial support. Funding that facilitated time on a research trip to develop the basis for this review was provided by a Universities of Manchester and Melbourne Research Fund Grant 'A Southern Hemisphere perspective on human-environment relations along desert margins.'

Competing interests. The authors declare none.

References

Abouelmagd A, Sultan M, Sturchio NC, Soliman F, Rashed M, Ahmed M, Kehew AE, Milewski A and Chouinard K (2017) Paleoclimate record in the Nubian sandstone aquifer, Sinai peninsula, Egypt. *Quaternary Research* **81**(1), 158–167. https://doi.org/10.1016/j.yqres.2013.10.017.

Al-Masrahy MA and Moutney NP (2015) A classification scheme for fluvial–aeolian system interaction in desert-margin settings. *Aeolian Research* **17**, 67–88. https://doi.org/10.1016/j.aeolia.2015.01.010.

Bar-Matthews M, Ayaloin A and Kaufman A (1997) Late quaternary Paleoclimate in the eastern Mediterranean region from stable isotope analysis of Speleothems at Soreq cave, Israel. *Quaternary Research* **47**(2), 155–168. https://doi.org/10.1006/qres.1997.1883.

Bateman MD, Bryant RG, Foster IDL, Livingstone I and Parsons AJ (2012) On the formation of sand ramps: A case study from the Mojave Desert. *Geomorphology* **161–162**, 93–109. https://doi.org/10.1016/j.geomorph.2012.04.004.

Beaudon E, Sheets JM, Martin E, Sierra-Hernández MR, Mosley-Thompson E and Thompson LG (2022) Aeolian dust preserved in the Guliya ice cap (Northwestern Tibet): A promising Paleo-environmental messenger. *Geosciences* **12**(10), 366. https://doi.org/10.3390/geosciences12100366.

Berger WH (2013) On the Milankovitch sensitivity of the quaternary deep-sea record. *Climate of the Past* **9**, 2003–2011. https://doi.org/10.5194/cp-9-2003-2013.

Beyer RM, Krapp M, Eriksson A and Manica A (2021) Climatic windows for human migration out of Africa in the past 300,000 years. *Nature Communications* **12**, 4889. https://doi.org/10.1038/s41467-021-24779-1.

Bond GC, Broecker WS, Johnsen S, McManus JF, Labeyrie L, Jouzel J and Bonani G (1993) Correlation between climate records from North Atlantic sediments and Greenland ice. *Nature* **365**, 143–147. https://doi.org/10.1038/365143a0.

Bond G, Showers W, Cheseby M, Lotti R, Almasi P, deMenocal P, Priore P, Cullen H, Hajdas I and Bonani G (1997) A pervasive millennial-scale cycle in North Atlantic Holocene and glacial climates. *Science* **278**(5341), 1257–1266. https://doi.org/10.1126/science.278.5341.1257.

Boyd M (2005) Phytoliths as paleoenvironmental indicators in a dune field on the northern Great Plains. *Journal of Arid Environments* **61**(3), 357–375. https://doi.org/10.1016/j.jaridenv.2004.09.015.

Braun DR, Levin NE, Stynder D, Herries AIR, Archer W, Forrest F, Roberts DL, Bishop LC, Matthews T, Lehmann SB, Pickering R and Fitzsimmons KE (2013) Mid-Pleistocene Hominin occupation at Elandsfontein, Western cape, South Africa. *Quaternary Science Reviews* **82**, 145–166. https://doi.org/10.1016/j.quascirev.2013.09.027.

Breeze PS, Groucutt HS, Drake NA, White TS, Jennings RP and Petraglia MD (2016) Palaeohydrological corridors for hominin dispersals in the Middle East similar to 250–70,000 years ago. *Quaternary Science Reviews* **144**, 155–185. https://doi.org/10.1016/j.quascirev.2016.05.012.

Broecker WS (1994) Massive iceberg discharges as triggers for global climate change. *Nature* **372**, 421–424. https://doi.org/10.1038/372421a0.

Broecker WS and Denton GH (1989) The role of ocean-atmosphere reorganizations in glacial cycles. *Geochimica et Cosmochimica Acta* **53**(10), 2465–2501. https://doi.org/10.1016/0016-7037(89)90123-3.

Burns SJ, Fleitmann D, Matter A, Neff U and Mangini A (2001) Speleothem evidence from Oman for continental pluvial events during interglacial periods. *Geology* **29**, 623–626. https://doi.org/10.1130/0091-7613(2001)029%3C0623:SEFOFC%3E2.0.CO;2.

Burrough SL, Thomas DSG and Singarayer JS (2009) Late quaternary hydrological dynamics in the middle Kalahari: Forcing and feedbacks. *Earth-Science Reviews* **96**, 313–326. https://doi.org/10.1016/j.earscirev.2009.07.001.

Cadd H, Williams AN, Saktura WM, Cohen TJ, Mooney SD, He C, Otto-Bliesner B and Turney CSM (2024) Last glacial maximum cooling induced positive moisture balance and maintained stable human populations in Australia. *Communications Earth & Environment* **5**(52), 1–10. https://doi.org/10.1038/s43247-024-01204-1.

Downloaded from https://www.cambridge.org/core. UNIVERSIDAD AUTONOMA METROPOLITANA, on 19 Nov 2026 at 18:47:39, subject to the Cambridge Core terms of use, available at https://www.cambridge.org/core/terms. https://doi.org/10.1017/dry.2025.10003

Chan EKF, Timmerman A, Baldi BF, Moore AE, Lyons RJ, Lee S-S, Kalsbeek AMF, Petersen DC, Rautenbach H, Förtsch HEA, Borman MSR, Hayes VM (2019) Human origins in a southern African palaeo-wetland and first migrations. *Nature* **575**, 185–189. https://doi.org/10.1038/s41586-019-1714-1

Chase BM (2009) Evaluating the use of dune sediments as a proxy for palaeo-aridity: A southern African case study. *Earth Science Reviews* **93**, 31–45. https://doi.org/10.1016/j.earscirev.2008.12.004.

Chase BM and Meadows ME (2007) Late quaternary dynamics of southern Africa's winter rainfall zone. *Earth Science Reviews* **84**, 103–138. https://doi.org/10.1016/j.earscirev.2007.06.002.

Chase BM, Quick LJ, Meadows ME, Scott L, Thomas DSG and Reimer PJ (2011) Late glacial interhemispheric climate dynamics revealed in south African hyrax middens. *Geology* **39**, 19–22. https://doi.org/10.1130/G31129.1.

Chase BM, Niedermeyer EM, Boom A, Carr AS, Chevalier M, He F, Meadows ME, Ogle N and Reimer PJ (2019) Orbital controls on Namib Desert hydroclimate over the past 50,000 years. *Geology* **47**(9), 867–871. https://doi.org/10.1130/G46334.1.

Cheng H, Li H, Sha L, Sinha A, Shi Z, Yin Q, Lu Z, Zhao D, Cai Y, Hu Y, Hao Q, Tian J, Kathayat G, Cong X, Zhoa J and Zhang H (2022) Milankovitch theory and monsoon. *The Innovation* **3**(6), 10038. https://doi.org/10.1016/j.xinn.2022.100338.

Clemens SC and Prell WL (2003) A 350,000 year summer-monsoon multi-proxy stack from the Owen ridge, northern Arabian Sea. *Marine Geology* **201** (1–3), 35–51. https://doi.org/10.1016/S0025-3227(03)00207-X.

Collins JA, Schefuß E, Govin A, Mulitza S and Tiedemann R (2014) Insolation and glacial–interglacial control on southwestern African hydroclimate over the past 140000 years. *Earth and Planetary Science Letters* **398**, 1–10. https://doi.org/10.1016/j.epsl.2014.04.034.

Colhoun EA, Pola JS, Barton CE and Heijnis H (1999) Late Pleistocene vegetation and climate history of Lake Selina, western Tasmania. *Quaternary International* **57–58**, 5–23.

Daniau A-L, Loutre M-F, Swingedouw D, Laepple T, Bassinot F, Malaizé B, Kageyama M, Charlier K and Carfantan H (2023) Precession and obliquity forcing of the south African monsoon revealed by sub-tropical fires. *Quaternary Science Reviews* **310**, 108128. https://doi.org/10.1016/j.quascirev.2023.108128.

Dansgaard W, Johnsen SJ, Clausen HB and Langway C (1972) Speculations about the next glaciation. *Quaternary Research* **2**, 396. https://doi.org/10.1038/s41561-022-00990-7.

Dansgaard W, Clausen HD, Gundestrup N, Hammer CU, Johnsen SF, Kristinsdottir PM and Reeh H (1982) A new Greenland deep ice core. *Science* **218**(4579), 1273–1277. https://doi.org/10.1126/science.218.4579.1273.

Dansgaard W, Johnsen SJ, Clausen HB, Dahl-Jensen D, Gundestrup NS, Hammer CU, Hvidberg CS, Steffense JP, Sveinbjörnsdottir AE, Jouzel J and Bond G (1993) Evidence for general instability of past climate from a 250-kyr ice-core record. *Nature* **364**, 218–220. https://doi.org/10.1038/364218a0.

Davies-Barnard T, Ridgwell A, Singarayer J and Valdes P (2017) Quantifying the influence of the terrestrial biosphere on glacial–interglacial climate dynamics. *Climate of the Past* **13**, 1381–1401.

De Deckker P, Moros M, Perner K, Blanz T, Wacker L, Schneider R, Barrows TT, O'Loingsigh T and Jansen E (2020) Climatic evolution in the Australian region over the last 94 ka – Spanning human occupancy -, and unveiling the last glacial maximum. *Quaternary Science Reviews* **249**, 106593. https://doi.org/10.1016/j.quascirev.2020.106593.

deMenocal PB (1995) Plio-Pleistocene African climate. *Science* **270**, 53–59. https://doi.org/10.1126/science.270.5233.53.

deMenocal PB (2004) African climate change and faunal evolution during the Pliocene-Pleistocene. *Earth and Planetary Science Letters* **220**, 3–24. https://doi.org/10.1016/S0012-821X(04)00003-2.

deMenocal PB and Tierney JE (2012) Green Sahara: African humid periods paced by earth's orbital changes. *Nature Education Knowledge* **3**(10), 12.

Denniston, Asmerom Y, Polyak VJ, Wanamaker AD, Jr, Ummenhofer CC, Humphreys WF, Cugley J, Woods D and Lucker S (2017) Decoupling of monsoon activity across the northern and southern indo-Pacific during the late glacial. *Quaternary Science Reviews* **176**, 101–105. https://doi.org/10.1016/j.quascirev.2017.09.014.

Di Nezio PN, Timmermann A, et al. (2016) The climate response of the indo-Pacific warm pool to glacial sea level. *Paleoceanography* **31**, 866–894. https://doi.org/10.1002/2015PA002890.

Dodson JR (1975) Vegetation history and water fluctuations at Lake Leake, south-eastern South Australia. II.50 000 B.P. To 10 000 B.P. *Australian Journal of Botany* **23**, 815–831.

Egbejule E (2024) Dramatic images show the first floods in the Sahara in half a century. *The Guardian* 11 Oct. https://www.theguardian.com/environment/2024/oct/11/dramatic-images-show-the-first-floods-in-the-sahara-in-half-a-century

Edmunds WM, Fellman E and Goni IB (1999) Lakes, groundwater and paleohydrology in the Sahel of NE Nigerai: Evidence from hydrogeochemistry. *Journal of the Geological Society of London* **156**, 45–355. https://doi.org/10.1144/gsjgs.156.2.0345.

Ehrmann E, Wilson PA, Arz HW, Shulz H and Schmiedl G (2024) Monsoon-driven changes in aeolian and fluvial sediment input to the Central Red Sea recorded throughout the last 200 000 years. *Climate of the Past* **20**, 37–52. https://doi.org/10.5194/cp-20-37-2024.

El-Shenawy MI, Kim S-T, Schwarcz HP, Asmerom Y and Polyak VJ (2018) Speleothem evidence for the greening of the Sahara and its implications for the early human dispersal out of sub-Saharan Africa. *Quaternary Science Reviews* **188**, 67–76. https://doi.org/10.1016/j.quascirev.2018.03.016.

Eriksson A, Betti L, Friend AD, Lycett SL, SIngarayer JS, von Cramon-Taubadel N, Valdes PJ, Ballouz F and Manica A (2012) Late Pleistocene climate change and the global expansion of anatomically modern humans. *Proceedings of the National Academy of Sciences of the United States of America* **109**, 16089–16094. https://doi.org/10.1073/pnas.1209494109.

Farber O and Kadmon R (2003) Assessment of alternative approaches for bioclimatic modeling with special emphasis on the Mahalanobis distance. *Ecological Modelling* **160**(1–2), 115–130. https://doi.org/10.1016/S0304-3800(02)00327-7.

Farmer EC, deMenocal PB and Marchitto TM (2005) Holocene and deglacial ocean temperature variability in the Benguela upwelling region: Implications for low-latitude atmospheric circulation. *Paleoceanography* **20**(2), PAS2018. https://doi.org/10.1029/2004PA001049.

Fleitmann D, Burns SJ, Pekala M, Mangini A, Al-Subbary A, Al-Aowah M, Kramers J and Matter A (2011) Holocene and Pleistocene pluvial periods in Yemen, southern Arabia. *Quaternary Science Reviews* **30**, 783–787. https://doi.org/10.1016/j.quascirev.2011.01.004.

Fitzsimmons KE, Cohen TJ, Hesse PP, Jansen J, Nanson GC, May T-H, Barrows T, Haberlah D, Hilgers A, Kelly T, Larsen J, Lomax J and Treble P (2013) Late quaternary palaeoenvironmental change in the Australian drylands. *Quaternary Science Reviews* **74**, 78–96. https://doi.org/10.1016/j.quascirev.2012.09.007.

Flint RF (1959) Pleistocene climates in eastern and southern Africa. *Bulletin of the Geological Society of America* **70**, 946–974.

Gale SJ, de Rochefort CA, Moore SR and Timms AJC (2017) The origin and stratigraphic significance of the quaternary Waterloo rock of the Botany Basin of south-East Australia. *Australian Geography* **49**, 291–316. https://doi.org/10.1080/00049182.2017.1398041.

Gasse F, Barker P, Gell PA, Fritz SC and Chalié F (1997) Diatom-inferred salinity in palaeolakes: An indirect tracers of climate change. *Quaternary Science Reviews* **16**, 547–563. https://doi.org/10.1016/S0277-3791(96)00081-9.

Gasse F, Chalie F, Vincens A, Williams MAJ and Williamson D (2008) Climatic patterns in equatorial and southern Africa from 30,000 to 10,000 years ago reconstructed from terrestrial and near-shore proxy data. *Quaternary Science Reviews* **27**, 2316–2340. 10.1016/j.quascirev.2008.08.027.

Geyh MA and Heine K (2014) Several distinct wet periods since 420 ka in the Namib Desert inferred from U-series dates of speleothems. *Quaternary Research* **81**, 381–391. https://doi.org/10.1016/j.yqres.2013.10.020.

Greve P, Roderick ML and Seneviratne SI (2017) Simulated changes in aridity from the last glacial maximum to 4xCO2. *Environmental Research Letters* **12**, 111021.

Groucutt HS, et al. (2021) Multiple hominin dispersals into Southwest Asia over the past 400,000 years. *Nature* **597**, 376–380. https://doi.org/10.1038/s41586-021-03863-y.

Guo ZT, Peng SZ, Hao QZ, Biscaye PE and Liu TS (2001) Origin of the Miocene–Pliocene red-earth formation at Xifeng in northern China and

Downloaded from https://www.cambridge.org/core. UNIVERSIDAD AUTONOMA METROPOLITANA, on 19 Nov 2026 at 18:47:39, subject to the Cambridge Core terms of use, available at https://www.cambridge.org/core/terms. https://doi.org/10.1017/dry.2025.10003

implications for paleoenvironments. *Palaeogeography, Palaeoclimatology, Palaeoecology* **170**(1–2), 11–26. https://doi.org/10.1016/S0031-0182(01)00235-8.

Guo ZT, Ruddiman WF, Hao QZ, Wu HB, Qiao YS, Zhu RZ, Peng SZ, Wei JJ, Yuan BY and Lui TS (2002) Onset of Asian desertification by 22 Myr ago inferred from loess deposits in China. *Nature* **416**, 159–163. https://doi.org/10.1038/416159a.

Harle KJ (1997) Late quaternary vegetation and climate change in southeastern Australia: Palynological evidence from marine core E55-6. *Palaeogeography Palaeoclimatology Palaeoecology* **131**, 465–483.

Harrison SP (1993) Late quaternary lake-level changes and climates of Australia. *Quaternary Science Reviews* **12**, 211–231. https://doi.org/10.1016/0277-3791(93)90078-Z.

Hays JD, Imbrie I and Shackleton NJ (1976) Variations in the earth's orbit: Pacemaker of the ice ages. *Science* **194**, 1121–1132. https://doi.org/10.1126/science.194.4270.1121.

Heinrich H (1988) Origin and consequences of cyclic ice rafting in the Northeast Atlantic Ocean during the past 130,000 years. *Quaternary Research* **29**, 142–152. https://doi.org/10.1016/0033-5894(88)90057-9.

Hemming SR (2004) Heinrich events: Massive late Pleistocene detritus layers of the North Atlantic and their global climate imprint. *Reviews of Geophyics* **42**(1), RG1005. https://doi.org/10.1029/2003RG000128.

Hesse PP (1994) The record of continental dust from Australia in Tasman Sea sediments. *Quaternary Science Reviews* **13**(3), 257–272. https://doi.org/10.1016/0277-3791(94)90029-9.

Hesse PP (2016) How do longitudinal dunes respond to climate forcing? Insights from 25 years of luminescence dating of the Australian desert dunefields. *Quaternary International* **410**, 11–29. https://doi.org/10.1016/j.quaint.2014.02.020.

Hodell DA and Channell JET (2016) Mode transitions in northern hemisphere glaciation: Co-evolution of millennial and orbital variability in quaternary climate. *Climate of the Past* **12**, 1805–1828. https://doi.org/10.5194/cp-18-249-2022.

Holden PB, Edwards NR, Rangel TF, Pereira EB, Tran GT and Wilkinson RD (2019) PALEO-PGEM v1.0: A statistical emulator of Pliocene–Pleistocene climate. *Geoscientific Model Development* **12**, 5137–5155. https://doi.org/10.5194/gmd-12-5137-2019.

Hua X and Wiens JJ (2013) How does climate influence speciation? *The American Naturalist* **182**, 1–12. https://doi.org/10.1086/670690.

Inkpen R and Wilson GP (2009) Explaining the past: Abductive and Bayesian reasoning. *Holocene* **19**, 329–334. https://doi.org/10.1177/0959683608100577.

Jamieson TF (1863) On the parallel roads of Glen Roy, and their place in the history of the glacial period. *Geological Society of London Quarterly Journal* **19**, 235–259.

Jankowski NR, Stern N, Lachlan TJ and Jacobs Z (2020) A high-resolution late quaternary depositional history and chronology for the southern portion of the Lake Mungo lunette, semi-arid Australia. *Quaternary Science Reviews* **233**, 106224. https://doi.org/10.1016/j.quascirev.2020.106224.

Jha DK, Patalano R, Ilgner J, Achyuthan H, Alsharekh AM, Armitage S, Blinkhorn J, Boivin N, Breeze PS, Devra R, Drake N, Groucutt HS, Guagnin M, Roberts P and Petraglia M (2024) Preservation of plant-wax biomarkers in deserts: Implications for quaternary environment and human evolutionary studies. *Journal of Quaternary Science* **39**(3), 349–358. https://doi.org/10.1002/jqs.3597.

Jiang QF, Shen J, Liu XQ, Zhang EL and Xiao XL (2007) A high-resolution climatic change since Holocene inferred from multi-proxy of lake sediment in westerly area of China. *Chinese Science Bulletin* **52**, 1970–1979. https://doi.org/10.1007/s11434-007-0245-6.

Kele S, Sallam ES, Capezzuoli A, Rogerson M, Wanas H, Shen C-C, Lone MA, Yu T-S, Schauer A and Huntington KW (2021) Were springline carbonates in the Kurkur–Dungul area (southern Egypt) deposited during glacial periods? *Journal of the Geological Society of London* **178**, jgs2020–jgs2147. https://doi.org/10.1144/jgs2020-147.

Kim J-H and Schneider RR (2003) Low-latitude control of interhemispheric sea-surface temperature contrast in the tropical Atlantic over the past 21 kyr: The possible role of SE trade winds. *Climate Dynamics* **21**, 337–347. https://doi.org/10.1007/s00382-003-0341-5.

Kutzbach JE (1981) Monsoon climate of the early Holocene: Climate experiment with the earth's orbital parameters for 9000 years ago. *Science* **214**, 59–61. https://doi.org/10.1126/science.214.4516.59.

Kutzbach JE, Guan J, He F, Cohen AS, Orland IJ and Chen G (2020) African climate response to orbital and glacial forcing in 140,000-y simulation with implications for early modern human environments. *PNAS* **117**(5), 2255–2264. https://doi.org/10.1073/pnas.1917673117.

Lambert F, Bigler M, Steffensen JP, Hutterli M and Fischer H (2012) Centennial mineral dust variability in high-resolution ice core data from dome C, Antarctica. *Climate of the Past* **8**, 609–623. https://doi.org/10.5194/cp-8-609-2012.

Larrasoaña JC, Roberts AP and Rohling EJ (2013) Dynamics of green Sahara periods and their role in Hominin evolution. *PLoS One* **8**(10), e76514. https://doi.org/10.1371/journal.pone.0076514.

Lisiecki LE and Raymo ME (2005) A Pliocene-Pleistocene stack of 57 globally distributed benthic d18O records. *Paleoceanography* **20**, PA1003. https://doi.org/10.1029/2004PA001071.

Laskar J, Robutel P, Joutel F, Gastineau M, Correia ACM and Levrard B (2004) A long term numerical solution for the insolation quantities of the earth. *Astronomy and Astrophysics* **428**(1), 261–285. https://doi.org/10.1051/0004-6361:20041335.

Liu B and Coulthard TJ (2015) Mapping the interactions between rivers and sand dunes: Implications for fluvial and aeolian geomorphology. *Geomorphology* **231**, 246–257. https://doi.org/10.1016/j.geomorph.2014.12.011.

Liu S, Jiang D and Lang Z (2018) A multi-model analysis of moisture changes during the last glacial maximum. *Quaternary Science Reviews* **191**, 363–377. https://doi.org/10.1016/j.quascirev.2018.05.029.

Liu S, Jiang D and Lang X (2019) Mid-Holocene drylands: A multi-model analysis using Paleoclimate modelling Intercomparison project phase III (PMIP3) simulations. *The Holocene* **29**(9), 1425–1438. https://doi.org/10.1177/0959683619854512.

Liu S, Jiang D and Lang Z (2021) Time-varying responses of dryland aridity to external forcings over the last 21 ka. *Quaternary Science Reviews* **262**, 106989. https://doi.org/10.1016/j.quascirev.2021.106989.

Lomax J, Hilgers A and Radtke U (2011) Palaeoenvironmental change recorded in the palaeodunefields of the western Murray Basin, South Australia – New data from single grain OSL-dating. *Quaternary Science ReviewsQuat. Sci. Rev.* **30**(5–6), 723–736. https://doi.org/10.1016/j.quascirev.2010.12.015

Manabe S and Hahn DG (1977) Simulation of the tropical climate of an ice age. *Journal of Geophysical Research* **82**(27), 3889–3911. https://doi.org/10.1029/JC082i027p03889.

Marshall AG and Lynch AH (2006) Time-slice analysis of the Australian summer monsoon during the late quaternary using the Fast Ocean atmosphere model. *Journal of Quaternary Science* **21**, 789–801. https://doi.org/10.1002/jqs.1063.

Milankovitch M (1920) *Theorie Mathematique Des Phenomenes Thermiques Produits Par la Radiation Solarie*. Paris: Gaultier-Villars

Miller GH, Magee JW and Jull AJT (1997) Low-latitude glacial cooling in the southern hemisphere from amino-acid racemization in emu eggshells. *Nature* **385**, 241–244. https://doi.org/10.1038/385241a.

Magee JW and Miller GH (1998) Lake Eyre palaeohydrology from 60 ka to the present: Beach ridges and glacial maximum aridity. *Palaeogeography Palaeoclimatology Palaeoecology* **144**, 307–329. https://doi.org/10.1016/S0031-0182(98)00124-2.

Mondanara A, Melchionna M, Di Febbraro M, Castiglione S, Holden PB, Edwards NR, Carotenuto F, Mairana L, Modafferi M, Serio C, Diniz-Filho JAF, Rangel T, Rook L, O'Higgins P, Spikins P, Profico A and Raia P (2020) A major change in rate of climate niche envelope evolution during hominid history. *iScience* **23**, 101693. https://doi.org/10.1016/j.isci.2020.101693.

Mercader J, Akuku P, Boivin N, Camacho A, Carter T, Clarke S, Temprana AC, Favreau J, Galloway J, Hernando R, Haung H, Hubbard S, Kaplan JO, Larter S, Magohe S, Mohamed A, Mwanbwiga A, Oladele A, Petraglia M, Roberts P, Saladi P, Shikoni A, Silva R, Soto M, Stricklin D, Mekonnen DZ, Zhao W and Durkin P (2025) *Homo erectus* adapted to steppe-desert climate extremes one million years ago. *Communications Earth & Environment* **6**, 1. https://doi.org/10.1038/s43247-024-01919-1.

Nash DJ (2022a) Dry valleys (*Mekgacha*). In Eckardt FD (ed), *Landscapes and Landforms of Botswana, World Geomorphological Landscapes*. Switzerland: Springer Nature, pp. 179–199. https://doi.org/10.1007/978-3-030-86102-5_11

Downloaded from https://www.cambridge.org/core. UNIVERSIDAD AUTONOMA METROPOLITANA, on 19 Nov 2026 at 18:47:39, subject to the Cambridge Core terms of use, available at https://www.cambridge.org/core/terms. https://doi.org/10.1017/dry.2025.10003

Nash DJ (2022b) Calcretes, silcretes and intergrade duricrusts. In Eckardt FD (ed), *Landscapes and Landforms of Botswana World Geomorphological Landscapes*. Switzerland: Springer Nature, pp. 223–246. https://doi.org/10.1007/978-3-030-86102-5_13

Nicholson SL, **Pike AW**, **Hosffeld R**, **Roberts N**, **Sahy D**, **Woodhead J**, **Cheng H**, **Edwards RL**, **Affolter S and Leuenberger M** (2020) Pluvial periods in southern Arabia over the last 1.1 million-years. *Quaternary Science Reviews* **229**(2020), 106112. https://doi.org/10.1016/j.quascirev.2019.106112.

Nitundil S, **Stone A and Srivistava A** (2023) Applicability of using portable luminescence reader for rapid age-assessments of dune accumulation in the Thar desert, India. *Quaternary Geochronology* **78**, 101468. https://doi.org/10.1016/j.quageo.2023.101468.

Otto-Bliesner BL, **Braconnot P**, **Harrison SP**, **Lunt DJ**, **Abe-Ouchi A**, **Albani S**, **Bartlein PJ**, **Capron E**, **Carlson AE**, **Dutton A**, **Fischer H**, **Goelzer H**, **Govin A**, **Haywood A**, **Joos F**, **LeGrande AN**, **Lipscomb WH**, **Lohmann G**, **Mahowald N**, **Nehrbass-Ahles C**, **Pausata FSR**, **Peterschmitt J-Y**, **Phipps SJ**, **Renssen H and Zhang Q** (2017) The PMIP4 contribution to CMIP6 – Part 2: Two interglacials, scientific objective and experimental design for Holocene and last interglacial simulations. *Geoscientific Model Development* **10**, 3979–4003. https://doi.org/10.5194/gmd-11-1033-2018.

Parmenter C and Folger DW (1974) Eolian biogenic detritus in deep sea sediments: A possible index of equatorial ice age aridity. *Science* **185**, 695–698. https://doi.org/10.1126/science.185.4152.695.

Partridge TC, **deMenocal PB**, **Lorentz SA**, **Paiker MJ and Vogel JC** (1997) Orbital forcing of climate over South Africa: A 200,000-year rainfall record from the Pretoria saltpan. *Quaternary Science Reviews* **16**(10), 1125–1133. https://doi.org/10.1016/S0277-3791(97)00005-X.

Passarge S (1904) *Die Kalahari*. Berlin: Dietrich Reimer, p. 822

Paillou P, **Lopez S**, **Marais E and Scipal K** (2020) Mapping Paleohydrology of the ephemeral Kuiseb River, Namibia, from radar remote sensing. *Water* **12** (15), 1411. https://doi.org/10.3390/w12051441.

Petherick L, **McGowan H and Moss P** (2008) Climate variability during the last glacial maximum in eastern Australia: Evidence of two stadials? *Journal of Quaternary Science* **23**(8), 787–802. https://doi.org/10.1002/jqs.1186.

Petherick L, **Bostock H**, **Cohen TJ**, **Fitzsimmons K**, **Tibby J**, **Fletcher M-S**, **Moss P**, **Reeves J**, **Mooney S**, **Barrows T**, **Kemp J**, **Jansen J**, **Nanson G and Dosseto A** (2013) Climatic records over the past 30 ka from temperate Australia – A synthesis from the Oz-INTIMATE workgroup. *Quaternary Science Reviews* **74**, 58–77. https://doi.org/10.1016/j.quascirev.2012.12.012.

Petit JR, **Briat M and Royer A** (1981) Ice age aerosol content from East Antarctic ice core samples and past wind strength. *Nature* **293**, 391–394. https://doi.org/10.1038/293391a0.

Petit JR, **Jouzel J**, **Raynaud D**, **Barkov N**, **Barnola J-M**, **Basile I**, **Bender ML**, **Chappellaz JA**, **Davis JC**, **Delaygue G**, **Delmotte M**, **Kotlyakov V**, **Legrand MR**, **Lipenkov VY**, **Lorius C**, **Pepin L**, **Ritz C**, **Saltzman ES and Stiévenard M** (1999) Climate and atmospheric history of the past 420,000 years from the Vostok ice core, Antarctica. *Nature* **399**(6735), 429–436. https://doi.org/10.1038/20859.

Picart C, **Dauteuil O**, **Pickford M and Owono FM** (2020) Cenozoic deformation of the south African plateau, Namibia: Insights from planation surfaces. *Geomorphology* **35**, 106922. https://doi.org/10.1016/j.geomorph.2019.106922.

Pisias NG and Moore TC (1981) The evolution of Pleistocene climate: A time series approach. *Earth and Planetary Science Letters* **52**(2), 450–458. https://doi.org/10.1016/0012-821X(81)90197-7.

Prentice IC, **Villegas-Diaz R and Harrison SP** (2022) Accounting for atmospheric carbon dioxide variations in pollen-based reconstruction of past hydroclimates. *Global and Planetary Change* **211**, 103790. https://doi.org/10.1016/j.gloplacha.2022.103790.

Raia P, **Mondanaro A**, **Melchionna M**, **Di Febbraro M and Diniz-Filho JAF** (2020) Past extinctions of *homo* species coincided with increased vulnerability to climatic change. *One Earth* **3**, 1–11. https://doi.org/10.1016/j.oneear.2020.09.007.

Raymo ME, **Rind D and Ruddiman WF** (1990) Climatic effects of reduced Arctic Sea ice limits in the GISS-II general circulation model. *Paleoceanography and Paleoclimatology* **5**(3), 367–382. https://doi.org/10.1029/PA005i003p00367.

Rohling EJ, **Marino G and Grant KM** (2015) Mediterranean climate and oceanography, and the periodic development of anoxic events (sapropels). *Earth Science Reviews* **143**, 62–97. https://doi.org/10.1016/j.earscirev.2015.01.008.

Roberts AP, **Rohling EJ**, **Grant KM**, **Larrasoaña JC and Liu Q** (2011) Atmospheric dust variability from Arabia and China over the last 500,000 years. *Quaternary Science Reviews* **30**, 3537–3541. https://doi.org/10.1016/j.quascirev.2011.09.007.

Roberts P and Stewart BA (2018) Defining the 'generalist specialist' niche for Pleistocene *Homo sapiens*. *Nature Human Behaviour* **2**, 542–550. https://doi.org/10.1038/s41562-018-0394-4.

Robins L, **Roskin J**, **Marder O**, **Edeltin L**, **Yu L and Greenbaum N** (2023) Geomorphic, environmental, and archeological significance of last glacial maximum to middle Holocene dune damming, northwestern Negev dunefield margin, Israel. *Quaternary Science Reviews* **308**, 108098. https://doi.org/10.1016/j.quascirev.2023.108098.

Rogerson M, **Dublyansky Y**, **Hoffman DL**, **Luetscher M**, **Töchterle P and Spötl C** (2019) Enhanced Mediterranean water cycle explains increased humidity during MIS 3 in North Africa. *Climate of the Past* **15**, 1757–1769. https://doi.org/10.5194/cp-15-1757-2019.

Rousseau DD, **Boers N**, **Sima A**, **Svensson A**, **Bigler M**, **Lagroix F**, **Taylor S and Antoine P** (2017) MIS3 & 2 millennial oscillations in Greenland dust and Eurasian aeolian records – A paleosol perspective. *Quaternary Science Reviews* **169**, 99–113. https://doi.org/10.1016/j.quascirev.2017.05.020.

Rowell A, **Thomas D**, **Bailey R**, **Stone A**, **Garzanti E and Padoan M** (2017) Controls on sand ramp formation in southern Namibia. *Earth Surface Processes and Landforms* **43**(1), 150–171. https://doi.org/10.1002/esp.4159.

Ruddiman WF (2006) Orbital changes and climate. *Quaternary Science Reviews* **25**(23024), 3092–3112. https://doi.org/10.1016/j.quascirev.2006.09.001.

Ruddiman WF, **Raymo M and McIntyre A** (1986) Matuyama 41,000-year cycles: North Atlantic Ocean and northern hemisphere ice sheets. *Earth and Planetary Science Letters* **80**, 117–129. https://doi.org/10.1016/0012-821X(86)90024-5.

Sarnthein M (1977) Sand deserts during glacial maximum and climatic optimum. *Nature* **272**, 43–46. https://doi.org/10.1038/272043a0

Scerri EML, **Thomas MG**, **Manica S**, **Gunz P**, **Stock JT**, **Stringer C**, et al. (2018) Did our species evolve in subdivided populations across Africa, and why does it matter? *Trends in Ecology & Evolution* **33**, 582–594. https://doi.org/10.1016/j.tree.2018.05.005.

Scheff J, **Seager R**, **Liu H and Coats S** (2017) Are glacials dry? Consequences for paleoclimatology and for greenhouse warming. *Journal of Climate* **30**, 6593–6609. https://doi.org/10.1175/JCLI-D-16-0854.1.

Shi N, **Schneider R**, **Beug H-J and Dupont LM** (2001) Southeast trade wind variations during the last 135 kyr: Evidence from pollen spectra in eastern South Atlantic sediments. *Earth and Planetary Science Letters* **187**(3–4), 311–321. https://doi.org/10.1016/S0012-821X(01)00267-9.

Simon MH, **Ziegler M**, **Bosmans J**, **Barker S**, **Reason CJC and Hall IR** (2015) Eastern south African hydroclimate over the past 270,000 years. *Scientific Reports* **5**, 18153. https://doi.org/10.1038/srep18153.

Skonieczny C, **Paillou P**, **Bory A**, **Bayon G**, **Biscara L**, **Crosta X**, **Eynaud F**, **Malaizé B**, **Revel M**, **Aleman N**, **Barusseau J**, **Vernet R**, **Lopez S and Grousset F** (2015) African humid periods triggered the reactivation of a large river system in Western Sahara. *Nature Communications* **6**(1), 8751. https://doi.org/10.1038/ncomms9751.

Skonieczny C, **McGee D**, **Winckler G**, **Bory A**, **Bradtmiller I**, **Kinsley CW**, **Polissar PJ**, **De Pol-Holz R**, **Rossignol L and Malaize B** (2019) Monsoon-driven Saharan dust variability over the past 240,000 years. *Science Advances* **5**, eeav1887. https://doi.org/10.1126/sciadv.aav1887.

Smith GI (2009) *Late Cenozoic Geology and Lacustrine History of Searles Valley, Inyo and San Bernadino Counties*, Vol. **1727**. California: U.S. Geological Survey Professional Paper

Srivastava P, **Brook GA and Marais E** (2005) Depositional environment and luminescence chronology of the Hoarusib River clay castles sediments, northern Namib Desert, Namibia. *Catena* **59**, 187–204. https://doi.org/10.1016/j.catena.2004.06.003.

Stone A (2014) Last glacial maximum conditions in southern Africa: Are we any closer to understanding the climate of this time period. *Progress in Physical Geography* **38**(5), 1–24. https://doi.org/10.1177/0309133314528943.

Stone A (2021) Dryland dunes and other dryland environmental archives as proxies for late quaternary stratigraphy and environmental and climate change in southern Africa. *Geological Society of South Africa* **124**, 927–962. https://doi.org/10.25131/sajg.124.0055.

Downloaded from https://www.cambridge.org/core. UNIVERSIDAD AUTONOMA METROPOLITANA, on 19 Nov 2026 at 18:47:39, subject to the Cambridge Core terms of use, available at https://www.cambridge.org/core/terms. https://doi.org/10.1017/dry.2025.10003

Stone A and Larsen J (2011) The peaks and troughs of dune records: (how much) should we worry about sampling resolution? In *XVIII INQUA Congress 2011, 21 July to 27 August 2011, Bern, Switzerland*.

Stone A and Thomas DSG (2008) Linear dune accumulation chronologies from the southwest Kalahari, Namibia: Challenges of reconstructing late quaternary palaeoenvironments from aeolian landforms. *Quaternary Science Reviews* **27**(17–18), 1667–1681. https://doi.org/10.1016/j.quascirev.2008.06.008.

Stone A, Inglis RH, Candy I, Sahy D, Jourdan A-L, Barfod DN and Alsharekh AM (2023) Humid phases on the southwestern Arabian Peninsula are consistent with the last two interglacials. *Quaternary Science Reviews* **319**, 108333. https://doi.org/10.1016/j.quascirev.2023.108333.

Stute M and Talma AS (1997) Glacial temperatures and moisture transport regimes reconstructed from noble gases and 5180, Stampriet aquifer, Namibia. In *Isotope Techniques in the Study of Environmental Change, Proceedings of a Symposium*, International Atomic Energy Agency (IAEA), Vienna (Austria).

Stuut J-B, Prins MA, Schneider RR, Weltje GJ, Jansen JHF and Postma G (2002) A 300-kyr record of aridity and wind strength in southwestern Africa: Inferences from grain-size distributions of sediments on Walvis ridge, SE Atlantic. *Marine Geology* **180**, 221–233. https://doi.org/10.1016/S0025-3227(01)00215-8.

Telfer M and Hesse P (2013) Palaeoenvironmental reconstructions from linear dunefields: Recent progress, current challenges and future directions. *Quaternary Science Reviews* **78**, 1–21. https://doi.org/10.1016/j.quascirev.2013.07.007.

Telfer M and Thomas DSG (2006) Complex Holocene lunette dune development, South Africa: Implications for palaeoclimate and models of pan development in arid regions. *Geology* **34**, 835–856. https://doi.org/10.1130/G22791.1.

Teller JT, Rutter N and Lancaster N (1990) Sedimentology and palaeohydrology of late quaternary lake deposits in the northern Namib Sand Sea, Namibia. *Quaternary Science Reviews* **9**, 343–364. https://doi.org/10.1016/0277-3791(90)90027-8.

Thomas DSG and Burrough SL (2012) Interpreting geoproxies of late quaternary climate change in African drylands: Implications for understanding environmental change and early human behaviour. *Quaternary International* **253**, 5–17. https://doi.org/10.1016/j.quaint.2010.11.001.

Thomas DSG, Bailey R, Shaw PA, Durcan JA and Singarayer JS (2009) Late quaternary highstands at Lake Chilwa, Malawi: Frequency, timing and possible forcing mechanisms in the last 44 ka. *Quaternary Science Reviews* **28**(5–6), 526–539. https://doi.org/10.1016/j.quascirev.2008.10.023.

Tierney JE and deMenocal PB (2013) Abrupt shifts in horn of Africa Hydroclimate since the last glacial maximum. *Science* **342**(6160), 843–846. https://doi.org/10.1126/science.1240411.

Tierney JE, deMenocal PB and Zander PD (2017) A climatic context for the out-of-Africa migration. *Geology* **45**(11), 1023–1026. https://doi.org/10.1130/G39457.1.

Timmerman A and Friedrich T (2016) Late Pleistocene climate drivers of early human migration. *Nature* **538**, 92–95. https://doi.org/10.1038/nature19365.

Timmerman A, Yun K-S, Raia P, Ruan J, Mondanar A, Zeller E, Zolikofer C, Ponce de León M, Lemmon D, Willeit M and Ganopolsji A (2022) Climate effects on archaic human habitats and species successions. *Nature* **604**, 495–501. https://doi.org/10.1038/s41586-022-04600-9.

Timmerman A, Raia P, Mondanaro A, Zollikofer CPE, de León MP, Zeller E and Yun K-S (2024) Past climate change effects on human evolution. *Nature Reviews Earth & Environment* **5**, 701–716. https://doi.org/10.1038/s43017-024-00584-4.

Turnbull M, Parker AG and Janowski NR (2023) The history of phytolith research in Australasian archaeology and palaeoecology. *Vegetation History and Archaeobotony* **32**, 655–677. https://doi.org/10.1007/s00334-023-00922-4.

Vaks A, Bar-Matthews M, Matthews A, Ayalon A and Frumkin A (2010) Middle-late quaternary paleoclimate of northern margins of the Saharan-Arabian Desert: Reconstruction from speleothems of Negev Desert, Israel. *Quaternary Science Reviews* **29**, 264702662. https://doi.org/10.1016/j.quascirev.2010.06.014.

Wang B and Ding Q (2008) Global monsoon: Dominant mode of annual variation in the tropics. *Dynamics of Atmospheres and Oceans* **39**, 165–168. https://doi.org/10.1016/j.dynatmoce.2007.05.002.

Wang PX, Wang B, Cheng H, Fasullo J, Gui Z, Kiefer T and Liu Z (2017) The global monsoon across time scales: Mechanisms and outstanding issues. *Earth Science Reviews* **174**, 84–121. https://doi.org/10.1016/j.earscirev.2017.07.006.

Weij R, Sniderman JM, Woodhead JD, Hellstrom JC, Brown JR, Drysdale RN, Reed E, Bourne S and Gordon J (2024) Elevated southern hemisphere moisture availability during glacial periods. *Nature* **626**, 319–326. https://doi.org/10.1038/s41586-023-06989-3.

Williams MAJ (1975) Late Pleistocene tropical aridity synchronous in both hemispheres? *Nature* **253**, 617–618. https://doi.org/10.1038/253617a0.

Williams AN, Veth P, Steffen W, Ulm S, Turney CSM, Phipps S, Smith M and Reeves J (2015) A continental narrative: Human settlement patterns and Australasian climate change over the last 35,000 years. *Quaternary Science Reviews* **123**, 91–112. https://doi.org/10.1016/j.quascirev.2015.06.018.

Williams MAJ (2022) When the land sings: Reconstructing prehistoric environments using evidence from quaternary geology and geomorphology, with examples drawn from fluvial environments in the Nile and son valleys. *Quaternary* **5**(3), 32. https://doi.org/10.3390/quat5030032.

Wolff EW, Chappellaz J, Blunier T, Rasmussen SO and Svensson A (2010) Millennial-scale variability during the last glacial: The ice core record. *Quaternary Science Reviews* **29**, 2828–2838. https://doi.org/10.1016/j.quascirev.2009.10.013.

Woor S, Thomas DSG, Durcan JA, Burrough SL and Parton A (2023) The aggradation of alluvial fans in response to monsoon variability over the last 400 ka in the Hajar Mountains, south-East Arabia. *Quaternary Science Reviews* **322**, 108384. https://doi.org/10.1016/j.quascirev.2023.108384.

Xu H, Wang T, Miao J, Chen J and Chen S (2020) The PMIP3 simulated climate changes over arid Central Asia during the mid-Holocene and last glacial maximum. *Acta Geologigca Sinicia (English Edition of the Bulletin of the Geological Society of China)* **94**(3), 725–742. https://doi.org/10.1111/1755-6724.14542.

Yun K-S, Timmerman A, Lee S-S, Willeit M, Ganopolski A and Jadhav J (2023) A transient coupled general circulation model (CGCM) simulation of the past 3 million years. Climate of the PastClim. *Past*. **19**, 1951–1974. https://doi.org/10.5194/cp-19-1951-2023.

Zan J, Louys J, Dennel R, Petraglia M, Ning W, Fang X, Zhang W and Hu Z (2024) Mid-Pleistocene aridity and landscape shifts promoted Palearctic hominin dispersals. *Nature Communications* **15**, 10279. https://doi.org/10.1038/s41467-024-54767-0.

Zeller E, Timmerman A, K-S Y, Raia P, Stein K and Ruan J (2023) Human adaptation to diverse biomes over the past 3 million years. *Science* **380**, 604–608. https://doi.org/10.1126/science.abq1288.

Zhou L, Jiang Z, Larrasoaña JC, Li S, Liu Q, Chen L, Yin Z, Lui W, Guan Y, Zhang Y and Hu Y (2024) Aridity record of the Arabian Peninsula for the last 200 kyr: Environmental magnetic evidence from the western equatorial Indian Ocena. *Quaternary Science Reviews* **341**, 108876. https://doi.org/10.1016/j.quascirev.2024.108876.

Downloaded from https://www.cambridge.org/core. UNIVERSIDAD AUTONOMA METROPOLITANA, on 19 Nov 2026 at 18:47:39, subject to the Cambridge Core terms of use, available at https://www.cambridge.org/core/terms. https://doi.org/10.1017/dry.2025.10003